SIMULATION OF
THE HEAT AND MASS TRANSFER
IN MEAT EMULSION PRODUCTS

by

OLAF ECKARDT

INDEPENDENT STUDY

(Mechanical Engineering)

at the

UNIVERSITY OF WISCONSIN - MADISON

1996

ABSTRACT

In the last few years the food industry has grown steadily and made a better understanding of thermal food processing more and more important. Modern equipment offers the possibility of better controlling and better monitoring of the smokehouse conditions as air temperature, relative humidity and air velocity. A better knowledge of the heat and mass transfer during thermal food processing is necessary to develop new processes that have a higher energy efficiency and that can switch to other product lines like full-fat, low-fat or non-fat products more easily.

The research on a continuous commercial smokehouse started several years ago to increase the efficiency of the thermal process of a new non-fat hot dog product. Meanwhile this product line has already been improved. The goal of this research is now to find a model for the whole thermal cooking process that can be used for al kinds of meat emulsion products using the parameter models developed in previous works. The simulation results are compared to measured data. Then the simulation model is used to examine the impact of the different parameters which have an impact on the process. And finally a multi-zone commercial smokehouse is simulated. Accounting for the limits in the different zones, steps are developed that improve the thermal process, decreasing the mass loss and the processing time.

iii

ACKNOWLEDGMENTS

Without the scholarship of the German Academic Exchange Service (DAAD) and without Professor Kabelac who organized this exchange program between Hannover and Madison I could not have come to Madison. I am grateful for this opportunity.

I thank my parents and grandparents for there love and financial support, they never failed believing in me.

I thank my academic advisors Prof. Beckman and Prof. Mitchell for there advise. Thanks to Annette and Steve who shared the evening hours in the lab with me. There friendship gave me strength to go on. I thank Pat for his support, Stefan for his computer assistants, Marion, Steve Z., Roger, Paul and all other labmates who make the time that I spend in the lap joyful and pleasant.

I thank Sybille who gave me support with her love, her letters and telephone calls. A special thank you also to my roommates Ingo and Kelly, for the nice evenings, the dinner and for shopping and cooking.

There are many other people not mentioned by name who made my time in Madison one of the greatest experience. Thank you.

TABLE OF CONTENTS

LIST OF FIGURES

Chapter 6

LIST OF TABLES

Chapter 6

NOMENCLATURE

Roman symbols

A	$[m^2]$	area
c	$[J/kg\ K]$	specific heat
C	$[-]$	dimensionless moisture content
D	$[m^2/s]$	diffusivity coefficient
D_{eff}	$[m^2/s]$	effective moisture diffusion coefficient
FP	$[-]$	fat to protein ratio
h	$[W/m^2K]$	heat transfer coefficient
$\Delta H\upsilon$	$[J/kg]$	heat of evaporation
i	$[-]$	node number
j	$[kg\ m^2/s]$	mass flux
k	$[W/mK]$	thermal conductivity
k_x	$[mole/m^2s]$	mass transfer coefficient; mole fraction driving force
k_p	$[kg/Pa\ m^2s]$	mass transfer coefficient; partial pressure driving force
L	$[m]$	length of the product
m	$[kg]$	mass
M	$[g/mole]$	molecular weight
N	$[-]$	total number of nodes
p	$[Pa]$	pressure
p_w	$[Pa]$	partial pressure of water
q	$[J/m^2K]$	heat flux
r	$[m]$	radial coordinate
RH	$[\%]$	relative humidity
t	$[s]$	time
T	$[K]$	Temperature
u	$[kg_m/kg_d]$	dry weight moisture concentration
v	$[m/s]$	velocity
V	$[m^3]$	volume

| x | [m] | rectangular coordinate |
| z | [m] | rectangular coordinate |

Greek symbols

α	[m^2/s]	thermal diffusivity
θ	[°]	angle in cylindrical coordinates
ρ	[kg/m^3]	Density
τ	[s]	time
ω	[kg$_m$/kg$_t$]	wet-weight moisture concentration (mass fraction)

Subscripts

d	conduction
d	referring to dry mass
db	dry bulb conditions
dp	dew point conditions
f	referring to fat
ini	referring to initial conditions
m	moisture
o	referring to initial moisture content
p	time step
p	protein
r	radial direction
s	surface condition
sat	saturation condition
surf	surface condition
t	total
v	convection
w	referring to water
wb	wet bulb conditions
∞	ambient conditions

CHAPTER ONE

INTRODUCTION

In this chapter the properties of meat emulsions are characterized. Furthermore the processing steps of a commercial smokehouse for the processing of cylindrical meat emulsions products are summarized. The following chapters will introduce the simulation model used in this work and show the impact of the parameters involved in this problem on the thermal process.

1.1 Background

A better understanding of the cooking process of food has become more and more important in the last few years. The development of industrial process operations increased and required a more detailed knowledge of the heat and mass transfer mechanisms during the cooking of the products. Many different phenomena occur in a cooking process such as the diffusion of water, the melting of fats, the denaturation of proteins and the evaporation of water. The cooking process is used to preserve the product, but also changes product properties like texture, color and taste. The complexity of the process has been studied in several institutions to find a model that allows the simulation of the cooking process making reasonable assumption to simplify the process.

The processing of meat emulsions will be the subject of this work. The main components of meat emulsion products are moisture, fat and protein. The weight percent of each component varies for the different kinds of meat emulsions like full fat, low fat and non fat emulsions.

Typical full fat emulsions contain about 50% moisture, 35% fat and 10% protein, while non fat emulsions can reach a moisture content of up to 85%. In addition to these main components other ingredients like salt, preservatives, non-meat proteins and spices are mixed into the emulsion.

1.2 Meat Emulsion Processing

The processing of meat emulsion products in a continuous smokehouse process consists of several operation steps. The row meat has to be grinded and chopped. The final meat emulsion is stuffed into casing and linked to sticks that carry the products through the thermal process which consists of a spraying, smoking, cooking and chilling zone. Finally the casing is removed.

The products travel through the zones on a conveyance chain that transports the product in loops through the smokehouse as sketched in Figure 1.1. The traveling time in each zone in the smokehouse process discussed in this work is about 12 min. Each zone is responsible for a different aspect of the cooking process.

The spray zone quickly brings the product temperature up to about 32°C (90°F) by spraying warm water on the product. in the end of this zone the water is allowed to evaporate to evaporate to get a dry product surface. Droplets on the surface would effect the final color of the surface.

The smoke zone gives the product its final taste. The smoke zone of the smokehouse discussed in this work uses smoke from burned wood chips. Newer processes uses liquid smoke, that decreases the time needed for this particular zone.
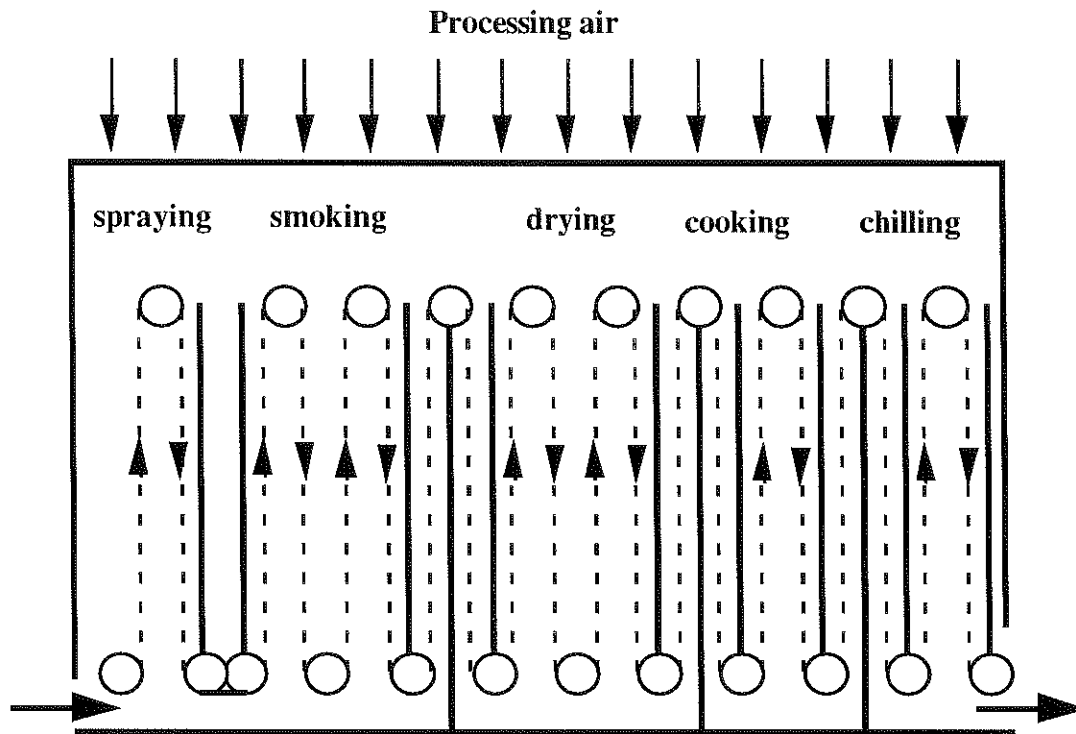
Figure 1.1: Schematic of a continuos smokehouse process with a vertical loop conveyor system for cylindrical meat emulsion products

The drying zone, or dry cooking zone gives the product its final texture. The product undergoes physical and chemical changes to form the hide that gives the product the "bit". Thus changes of the conditions in this zone are very limited, even for newer processes this zone will take seven to eight minutes.

The final cooking zone rises the product temperature to 68.3°C (155°F) to cook the product and to satisfy the standard health regulations.

4

The chilling zone reduces the product temperature to reduce product damage during packaging and to reduce the cooling load of the refrigerators. The cooling is accomplished by spraying chilled salt brine on the product.

CHAPTER TWO

REVIEW OF EXISTING MODELS

This chapter gives a short overview of existing models for meat emulsion properties. Most of the property data are listed in Table 2.1 .The models for the effective moisture diffusivity and the model for the isotherms that describe the equilibrium relationship of the moisture content at the product surface and the relative humidity in the process air are discussed explicitly.

2.1 Properties of Meat Emulsions

The properties of meat emulsion have been examined in previous researches. The different models are summarized in Table 2.1. The dependencies of several variables are not useful in all cases. Thus one should use constant values in those cases where the range of the variable is small and the impact of the variable on the whole process is not very significant. Common ranges of the values are also given in Table 2.1 and will be discussed later. The ranges given for the different properties cover the range of interest for this simulation. Property model which are only valid for a certain variable range are indicated.

2.2 Equilibrium at the surface

To simulate the heat and mass transfer within the product, the heat and mass transfer coefficients have to be calculated. Beside these transfer coefficients, the change of phase of the moisture form liquid moisture within the product to vaporized moisture in the process air has to be modeled mathematically. This is done by an expression that describes the equilibrium relative humidity above the surface as a function of the moisture content in the meat emulsion. Due to results reported by Mittal et al. [1981], the internal temperature in a thin slab of meat emulsion rises so quickly that an isothermal condition can be assumed at the product surface. Hence, even though the overall process is transient, equilibrium is assumed at the interface of product and process air.

Attempts that used a linear isotherm for the equilibrium relative humidity as a function of the moisture content failed in fitting the simulation data to existing measured data. Measurements by Igbeka and Blaisdell [1982] presented in Figure 2.1 show that the equilibrium isotherms are sigmoidal in shape. Due to the sigmoidal shape it is not possible to make a accurate curve fit over the whole range of the relative humidity. The equilibrium moisture contents at low relative humidities (11-43%) are seen to be almost constant. When the temperature is decreased the equilibrium moisture contents will also decrease. For high relative humidities the isotherms are very steep with a constant shift to higher relative humidities for a increasing temperature. For low relative humidities the temperature of the environment is the critical parameter, while for high relative humidities the relative humidity is the critical parameter.

Table 2.1 :   Property values for meat emulsions for different compositions and temperatures

Property	Range	Reference
Density [kg/m^3]		
$\rho = 1024$	$\omega_m = 0.576$ (full-fat)	Schaefer [1995]
$\rho_{dry} = 434$		Schaefer [1995]
$\rho = 1036$	$\omega_m = 0.870$ (non-fat)	Schaefer [1995]
$\rho_{dry} = 134$		Schaefer [1995]
Thermal conductivity [W/m-K]		
$k = 0.355$ to 0.468	$T < 25C$; $0.54 < \omega_m < 0.71$	Timbers [1982]
$k = 0.080 + 0.52\ \omega_m$	$0.392 < k < 0.496$; for $0.60 < \omega_m < 0.80$	Sweat [1975] [3]
Specific heat [kJ/kg-K]		
dry meat emulsion		
$c_d = 1.58$		Martin [1995]
water		
$c_w = \sum a_i\ T^i$, $i = 0 - 5$	$4112 < c_w < 4023$; for $278 < T\ [K] < 373$	Martin[1995][1]
meat emulsion		
$c = \omega_d\ c_d\ +\ \omega_w\ c_w$		Martin [1995]
$c = 3.6$	$T < 40C$	Agrawal [1976]
$c = \sum \omega_i\ c_i$		Hallström [1988][2]
$c = 1.675 + 2.5\ \omega_m$		Dickerson [1965]
$c = 1.60 + 2.6\ \omega_m + 0.015\ \omega_f\ T$		Hallström [1988]
Moisture diffusivity [m^2/hr]		
$D_{eff} = 0.3224 \ast 10-4\ T\ \exp(-0.3302\ FP - 3060.37/\ T)$, $T < 58$ C $D_{eff} = 0.232\ T\ \exp(-0.0414\ FP - 6246.6/\ T)$, $T > 58$ C $5e-11 < D_{eff} < 5e-10$; for $280 < T\ [K] < 350$ $1.0 < FP < 3.0$		Mittal [1982]
$D_{eff} = 0.0029\ \exp(-0.4419\ FP - 4892.7\ /\ T + 11.55\ C)$ $1e-9 > D_{eff} > 1e-13$; for $280 < T\ [K] < 350$ $1.0 < FP < 3.0$ $1.0 > C > 0.0$		Mittal [1981]

[1] $a_0 = 757.1, a_1 = -11.56, a_2 = 7.0838e-2, a_3 = -2.1655e-4, a_4 = 3.3019e-7, a_5 = -2.0088e-10$
[2] $c_w = 4.18$ kJ/kgK , $c_c = 1.42$ kJ/kgK , $c_p = 1.55$ kJ/kgK , $c_f = 1.67$ kJ/kgK
[3] restricted range for the wet-weight moisture concentration

8

The equilibrium moisture content can be described as a function of the vapor pressure over the surface of the product using the equation

$$p_{surf}(RH,T) = RH * p_{sat}(T) \qquad (2.1)$$

In Figure 2.2 the strong influence of the temperature on the equilibrium vapor pressure is shown, by substituting equation 4.1 into the data available for Figure 2.1. Since the vapor pressure in the process air can be assumed to be constant, the isotherms shown in Figure 2.2 are proportional to the driving force for the mass transfer.
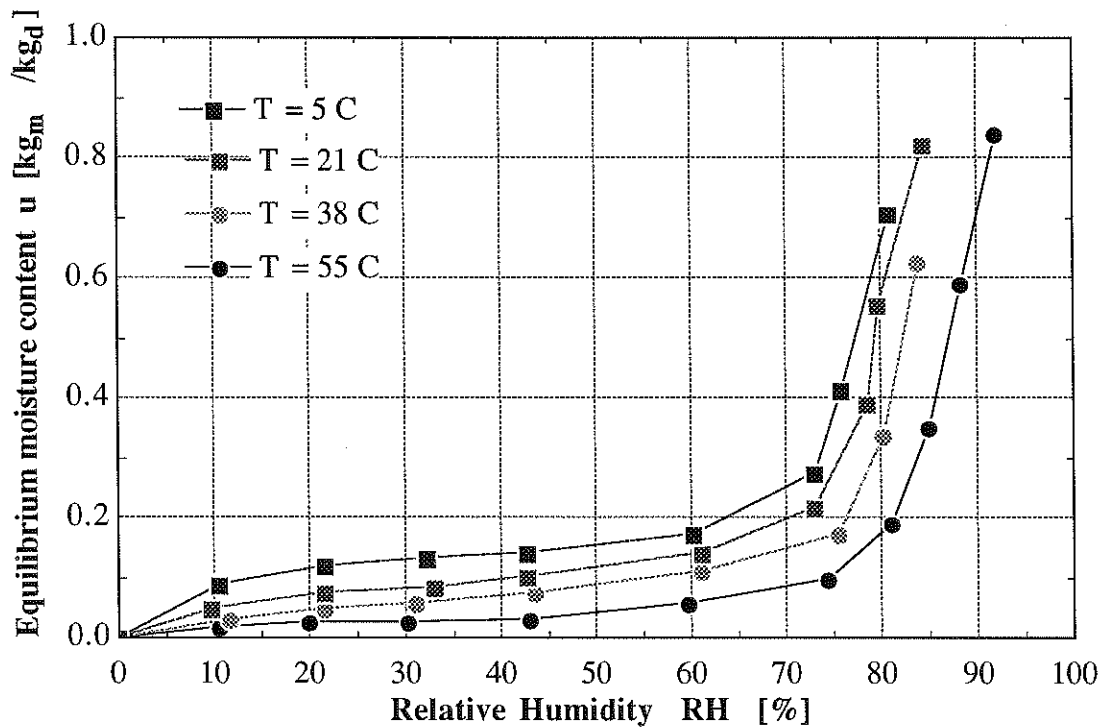
Figure 2.1 : Isotherms for meat emulsion measured by Igbeka and Blaisdell [1982].

The temperature and moisture content of the product varies over a wide range during the whole process. Hence, it is difficult to find a mathematical expression that account for

both, temperature and moisture variations. This is especially true for non-fat products which have a high initial water content of over 6 kg_m/kg_d. For a moisture contents over 0.8 no measured data are available. To make simulations possible, a constant maximum relative humidity is set for all moisture contents over 2.0 instead of using two function for high and low relative humidities.
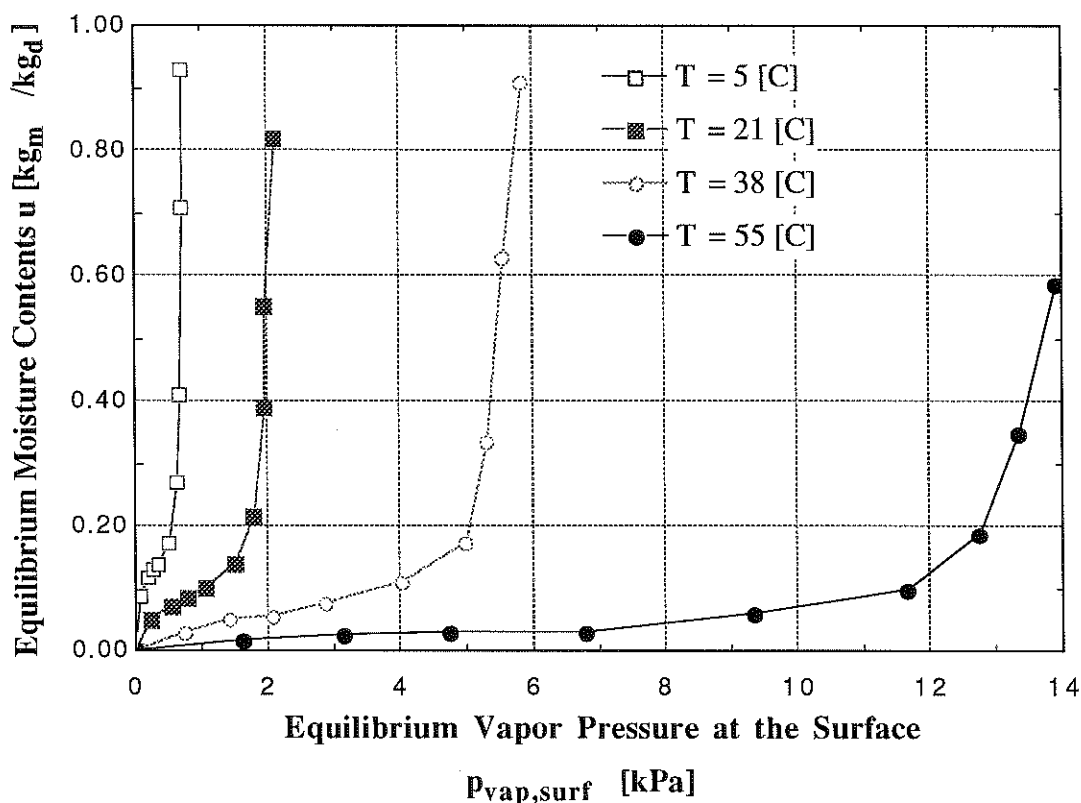
Figure 2.2: Equilibrium moisture contents as a function of the vapor pressure

2.3 Effective Moisture Diffusivity of Meat Emulsions

The effective moisture diffusivity is the material property that has the strongest impact on the thermal process of meat emulsion. Different models for the moisture diffusivity have been developed and used in previous researches. Two models developed by Mittal [1981,1982] are listed in Table 2.1. Model 1 describes the moisture diffusivity as a

function of the fat protein ratio (FP) and the temperature, model 2 describes the moisture diffusivity as a function of the FP ratio, the temperature and the dimensionless moisture content of the meat emulsion. Figure 2.3 and Figure 2.4 show the impact of the FP ratio on the moisture diffusivity for model 1 and model 2.
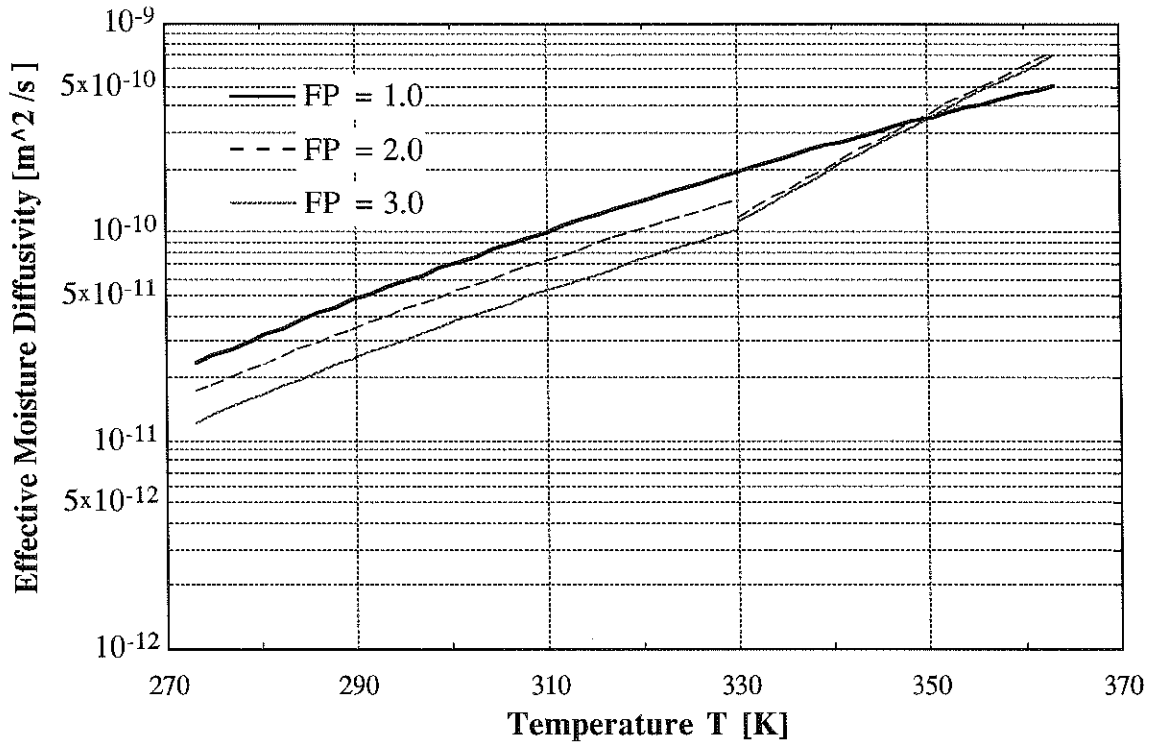
Figure 2.3 : Impact of the fat protein ratio (FP) on the moisture diffusivity for Model 1. The dimensionless moisture content for Figure 2.4 is assumed to be C = 0.6 .

Compared to the impact of the temperature the impact of the FP ratio is rather small for the common range of FP between one and three. Due to the high sensitivity of the process towards the moisture diffusivity even this impact should not be neglected.
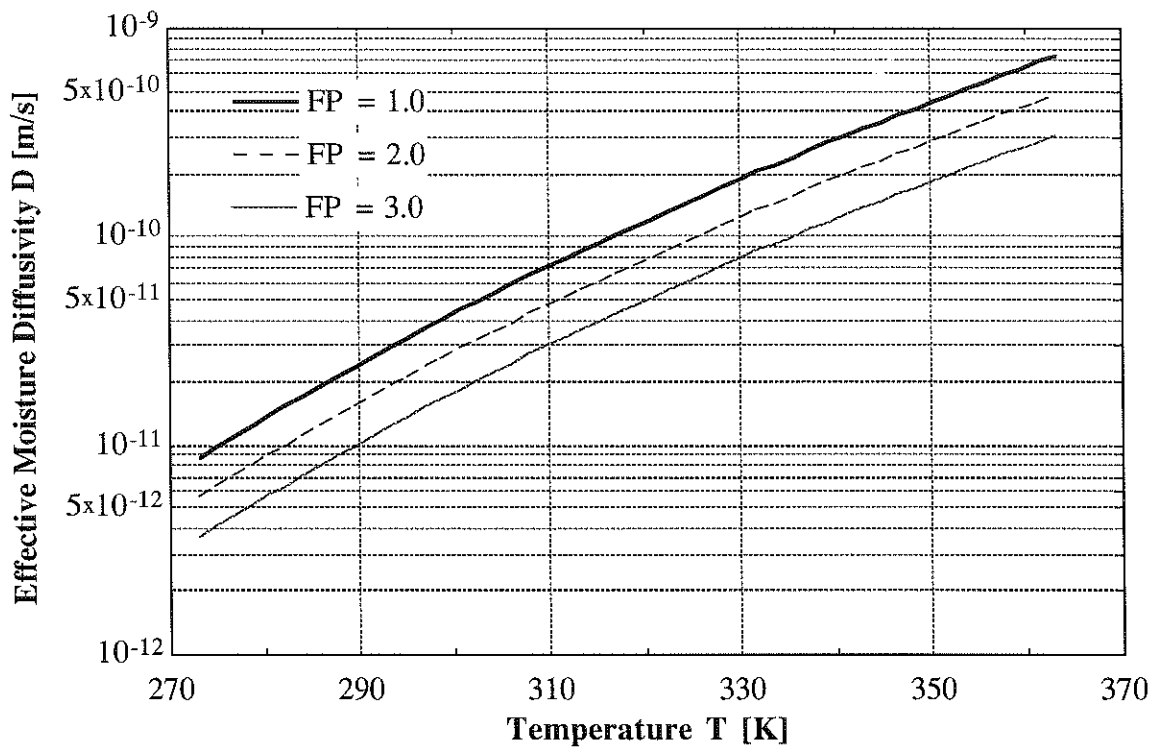
Figure 2.4 : Impact of the fat protein ratio (FP) on the moisture diffusivity for Model 2.

Figure 4.5 shows the impact of the dimensionless moisture content on the moisture diffusivity. Due to the definition of the dimensionless moisture content C the value for C will be unity in the beginning of the process and about 0.1 in the end for the process discussed in this work. So model 1 and model 2 will predict the opposite behavior of the moisture diffusivity during the whole process. While model 1 predicts an increasing moisture diffusivity as a result of the increasing temperature, model 2 predicts a decreasing moisture diffusivity because the decreasing dimensionless moisture diffusivity for model 2 has a much stronger impact on the diffusivity than the temperature. Comparing this two models for the moisture diffusivity already shows the large range of results calculated with the different models which could be found in the literature. To find a model that fit to the resent problem will be a major goal.
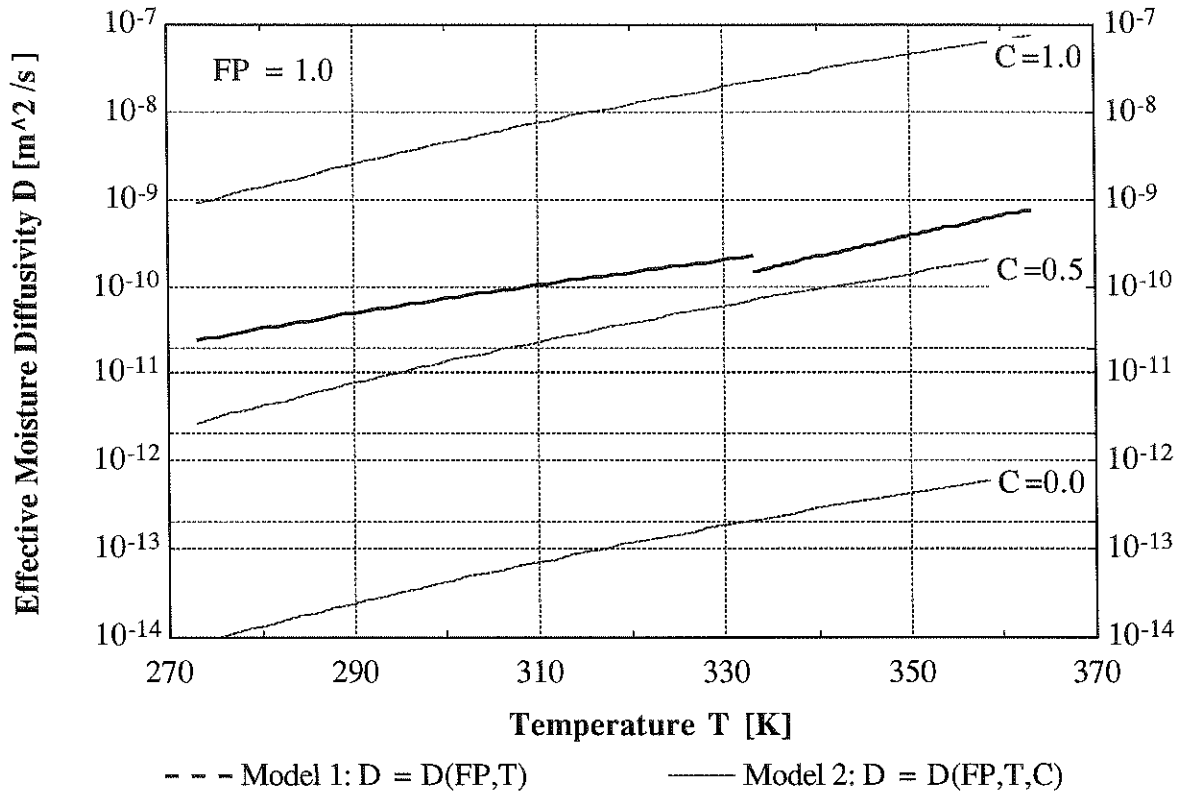
Figure 2.5: Impact of the dimensionless moisture content on the moisture diffusivity for Model 1 compared with Model 2.

Martin Schaefer [1995] has found the impact of several multiparameter models to be marginal compared with constant values for the moisture diffusivity that he calculated with a parameter estimation program. The values Schaefer calculated for the different meat emulsions are summarized in Table 2.2. The values for the effective moisture diffusion coefficient computed for the same compositions but samples from different batches range from 0.910e-10 to 2.52e-10 m^2/s for the full fat meat emulsion and from 1.77e-10 to 3.73e-10 m^2/s for the non fat meat emulsion.

The impact of different moisture diffusivities within this range will be investigated later and compared to the models mentioned above.

Table 2.2 :   Results calculated with a parameter estimation program reported by Martin

Schaefer [1995].

Relative Humidity	Meat emulsion	Moisture Diffusivity [m^2/s]	Meat emulsion	Moisture Diffusivity [m^2/s]
Sample 1 (small diameter products in cellulose casings)				
6.1%	full fat	2.24(±0.135)e-10	non fat	3.55(±0.341)e-10
15.6%	full fat	1.07(±0.098)e-10	non fat	2.52(±0.155)e-10
32.4%	full fat	1.13(±0.185)e-10	non fat	1.77(±0.109)e-10
	average	1.48e-10	average	2.61e-10
Sample 2 (medium diameter products in fibrous casings)				
7.1%	full fat	1.63(±0.203)e-10	-	
18.0%	full fat	0.910(±0.201)e-10	-	
-	average	1.27e-10	-	
Sample 3				
-	full fat	0.913(±0.151)e-10		
-	full fat	0.987(±0.121)e-10	non fat	3.73(±0.247)e-10
Sample 4				
-	full fat	2.52(±1.95)e-10		
-	-	-	low fat	2.36(±0.182)e-10

CHAPTER THREE

THE SIMULATION MODEL

This chapter will give a short overview of the fundamental equations used for the final simulation model. It will introduce the assumptions and boundary conditions and derive the final differential equations.

3.1 The Governing Equations for Heat and Mass Transfer

Two methods are used to formulate equations that describe the energy and the mass transfer of a system. The *shell energy balance* and the *equations of change*, both discussed in Bird, Stewart and Lightfoot [1960]. The *shell energy balance* is based on the conservation of energy and mass by looking at a differential shell. This method can be used for those systems that can be reduced to a two dimensional problem, so that the temperature or the mass flow in one dimension can be assumed to be constant. Using the *equations of change* the energy and mass balances are made for a differential element, accounting for all possible contributions. They are tabled in Bird, Stewart and Lightfoot [1960] for rectangular, cylindrical and spherical systems. One uses them by canceling all terms that do not match the system that needs to be analyzed.

One also applies Fourier's law for the heat transfer and Fick's law for the mass transfer. These equations show the analogy between the heat and the mass transfer

$$\textit{Fourier's law} \quad q \;=\; -\alpha \rho c \, \frac{\partial(T)}{\partial x} \qquad\qquad (3.1)$$

$$\textit{Fick's law} \quad j \;=\; -D \rho \, \frac{\partial \omega}{\partial x} \qquad\qquad (3.2)$$

Where q and j are the heat and the mass flux, T and ω are the temperature and the mass fraction, α and D are the thermal and the mass diffusivity and ρ and c are the density and the specific heat.

The equations of change for a one-dimensional cylindrical system for conduction only and the equivalent for mass flux will give the equations.

$$\rho c \frac{\partial T}{\partial \tau} \;=\; -\frac{1}{r} \frac{\partial}{\partial r} \left(r k \frac{\partial T}{\partial r} \right) \qquad\qquad (3.3)$$

$$\frac{\partial \omega}{\partial \tau} \;=\; \frac{1}{r} \frac{\partial}{\partial r} \left(r D \frac{\partial \omega}{\partial r} \right) \qquad\qquad (3.4)$$

The convective heat and mass transfer at the surface will not appear in the differential equations but in the boundary conditions as discussed later.

The mass fraction ω can be based on the wet-weight or the dry-weight. That are defined as:

dry-weight moisture concentration	$u_m \;=\; \rho_m / \rho_d$
wet-weight moisture concentration	$\omega_m \;=\; \rho_m / \rho$
total density	$\rho \;=\; \rho_m + \rho_d$

Where ρ_m and ρ_d are the moisture density and the dry density. ρ is the total density of the product. For drying processes Perry *et al.* [1984] suggest using the dry-weight moisture fraction, that expresses the moisture in a material as a percentage of the weight of the dry material. This is supposed to have the advantage that the change of moisture is constant for all moisture contents. If the moisture content is calculated with the wet-weight moisture concentration, referred to Perry *et al* [1984] "a 2 or 3 percent change at high moisture contents (above 70 percent) actually represents a 15 to 20 percent change in evaporative load". For lower moisture concentrations of about 20 percent it has been found that the difference is less. Using the wet-weight moisture contents the calculated total mass loss underestimates the moisture loss for about 3 to 6 percent for the thermal process calculated in this work.

To convert the wet-weight into the dry-weight concentration the following equations can be used:

$$u_m = \frac{\omega_m}{1 - \omega_m} \quad ; \quad \omega_m = \frac{u_m}{1 + u_m} \tag{3.5}$$

The physical process in the surface of a meat emulsion is primarily a drying process. So the dry-weight moisture concentration is used for the calculation of the moisture profile and the total moisture loss in this work.

3.2 The Simulation Model

3.2.1 Assumptions

The thermal process of meat emulsion is very complex because chemical processes, thermal processes and mass transfer take place at the same time. The following assumptions are made to simplify the process:

- The moisture in the product diffuses in liquid phase.

- The evaporating moisture does not change the volume of the product.

- The driving force for the moisture diffusion is the moisture concentration difference. A effective moisture diffusivity can bee used to correlate the difference of the moisture concentration to a moisture flux.

- The casings of the product have no effect on the heat transfer at the product surface. Using moisture permeable casings the resistance to mass transfer is negligible.

- End effects and circumferential variations of heat and mass transfer are negligible. Thus heat and mass transfer occurs only in the radial direction.

- Latent heat due to melting fats are small compared to the total heat flux and can be neglected.

- The heat and mass transfer between product and processing air does not change the temperature and humidity of the process air.

- Flux couplings, i.e. moisture gradients causing energy fluxes (Dufour effect) and temperature gradients causing moisture fluxes (Soret effect), are negligible.

A significant simplification for the derivation of the differential equation at this point is, that one can assume a one-dimensional heat and mass transfer in the meat emulsion. Martin

Schaefer [1995] calculated the impact of the circumferential variation of the local heat transfer coefficients for airflow normal to a cylinder and the corresponding temperature profiles over the cross section area of a cylinder. He found the circumferential variations of the temperature profile small enough to justify the assumption of a one-dimensional heat and mass transfer.

3.2.2 The Shell Balance Method for Simultaneous Heat and Mass Transfer

The shell balance method for the energy transfer on a infinite long cylindrical element of the thickness Δr for simultaneous heat and mass transfer gives the equation

$$\bar{\rho}\,\bar{c}\,\frac{\partial}{\partial \tau}\left(r\,\Delta\theta\,\Delta z\,\Delta r\,T\right) = r\,\Delta\theta\,\Delta z\,q_r\big|_r - r\,\Delta\theta\,\Delta z\,q_r\big|_{r+\Delta r}$$
$$+ r\,\Delta\theta\,\Delta z\,c_w j_w T\big|_r - r\,\Delta\theta\,\Delta z\,c_w j_w T\big|_{r+\Delta r}$$
(3.6)

The left hand side represents the change in internal energy with time. The first two terms on the right hand side represents the heat fluxes in an out of the control volume. The last two terms represent the enthalpy fluxes due to moisture diffusion in an out of the control volume. After converting this equation and substituting Fourier's law of heat conduction for q_r and Ficks's law of diffusion for j_w equation

$$\bar{\rho}\,\bar{c}\,\frac{\partial T}{\partial \tau} = \frac{1}{r}\frac{\partial}{\partial r}\left(r k\frac{\partial T}{\partial r} + r c_w \rho_d T D_{eff}\frac{\partial u}{\partial r}\right)$$
(3.7)

can be developed. Where u and T are the dry-weight moisture concentration and the temperature. The second term of equation 3.7 describes the enthalpy transport due to moisture diffusion. The mean density $\bar{\rho}$ and heat capacity $\bar{c}$ are defined as

$$\overline{\rho} = \rho_d + \rho_w \tag{3.8}$$

$$\overline{c} = \omega_d c_d + \omega_w c_w \tag{3.9}$$

The shell balance method for the mass transfer on a infinite long cylindrical element of the thickness Δr gives the equation

$$\overline{\rho}\,\overline{c}\frac{\partial}{\partial r}(r\,\Delta\theta\,\Delta z\,\Delta r\,u) = r\,\Delta\theta\,\Delta z\,j_w\big|_r - r\,\Delta\theta\,\Delta z\,j_w\big|_{r+\Delta r} \tag{3.10}$$

The left hand side represents the change in the moisture concentration with time. The right hand side represents the moisture diffusion in and out of the differential volume. Converting this equation and substituting Ficks's law of diffusion for j_w one can develop the equation

$$\frac{\partial u}{\partial \tau} = \frac{1}{r}\frac{\partial}{\partial r}\left(r\,D_{eff}\frac{\partial u}{\partial r}\right) \tag{3.11}$$

To solve the differential equations 3.7 and 3.11 one need the boundary conditions that are formulated in the following chapter.

3.3 The Boundary Conditions

Two sets of boundary conditions are necessary to solve the differential equation for heat transfer (equ.3.7) and the differential equation for mass transfer (equ.3.11). They are dependent on the assumptions made for the simulation model. Especially the boundary conditions for mass transfer will change with different assumptions as discussed in Chapter 2.2. Two different types of casings are used for meat emulsion processing, one allows

20

moisture transfer from the product to the process air and one is resistant to moisture transfer. Both types will be discussed. Equations 3.12 and 3.13 introduced in the following paragraphs are valid for both types of casings while the mass transfer coefficient k_p is zero for the moisture resistant casing.

The driving force for mass transfer is the concentration gradient. At the product surface the driving force is assumed to be the difference between the moisture concentration directly over the product surface $p_{w,s}$ and the moisture concentration in the process air $p_{w,\infty}$. Assuming the process air to be an ideal gas, the moisture concentration can be described with the relative humidity RH or the partial vapor pressure p_w of the process air. Using the partial vapor pressure the equation for mass transfer at the surface is

$$-\rho_d \, D_{eff} \frac{\partial u}{\partial r} \;=\; k_p \left(p_{w,s} \;-\; p_{w,\infty} \right) \tag{3.12}$$

where k_p is the mass transfer coefficient. Because the meat emulsion and the process air have different affinities to moisture (solid/gas), a coupling condition has to be used to convert the dry-weight moisture concentration in the meat emulsion u, to a equivalent partial vapor pressure at the product surface $p_{w,s}$. This transformation is the equilibrium relationship between moisture concentration in the product and relative humidity of the process air introduced in Chapter 2.2. Even though not very accurate for high temperatures the following curve fit to the measurements of Igbeka and Blaisdell [1982] together with Equation 2.1, are used for the calculations in this work

$$u_s \;=\; \sum_{i=1}^{5} a(i) \, RH^i \tag{3.13}^1$$

_____

[1] $a(1) = 1.0802,\quad a(2) = -8.3266,\quad a(3) = 30.65,\quad a(4) = -48.919,\quad a(5) = 28.408$

where u_s is the moisture content of the meat emulsion at the surface and RH is the equilibrium relative humidity over the surface.

If mass is transferred from the product to the processing air, the latent heat that needs to evaporate the moisture at the product surface is supplied by the processing air an the boundary condition for heat transfer can be written as

$$-k\frac{\partial T}{\partial r} \;=\; h\left(T_\infty - T_s\right) \;-\; \Delta \hat{H}_\upsilon\, k_p \left(p_{w,s} - p_{w,\infty}\right) \tag{3.14}$$

where h is the overall heat transfer coefficient, including radiation, and $\Delta \hat{H}_\upsilon$ is the latent heat of evaporation of water. The energy used for the evaporation of the moisture reduces the energy available to raise the product temperature. Evaporative cooling will occur if more energy is needed for evaporation than is transferred towards the product by convection.

Condensation of moisture vapor on the product surface from the process air will occur if the product surface temperature T_s is lower than the dew point temperature T_{dp} of the process air. This condensation period will especially occur in the beginning of the process when the product temperature is low and can be simulated in two different way:

- allowing mass transfer between process air and product in both directions;
- allowing mass transfer from the product to the process air only.

Mass transfer to the product will occur if the water vapor pressure over the surface of the product is lower than the water vapor pressure in the process air. The condensing vapor will raise the product temperature until the vapor pressure at the surface exceeds the vapor pressure of the process air and the direction of the mass transfer goes the opposite way. The simulation of this process is difficult because of the possibility that some or all of the water drips off the product due to gravity. It is hard to predict how many water will remain

22

on the casing and an adsorption isotherm would be need to model the condensation period. Thus this phenomena is not modeled in this work.

Only mass transfer from the product to the process air is allowed. The mass transfer coefficient k_p is set to zero if the vapor pressure at the product surface is lower than the vapor pressure of the process air. During this condensation period the heat transfer coefficient is very high. Thus the ratio of internal to external resistance is very high and one can assume that the temperature of the surface is equal to the dew point temperature of the process air. The temperature of the surface will stay at the dew point temperature as long as the convective heat flux q_v from the process air to the product surface is lower than the conductive heat flux q_d from the product surface towards the center. Without this additional statement the steep temperature gradient at the product surface would relax by decreasing the temperature of the surface and increasing the temperature of the center. In the next step the model would set the surface temperature back to the dew point temperature. This would lead to "back and forth" bouncing of the surface temperature.

Thus the temperature and moisture gradient within the product are assumed to be symmetrical, the temperature and moisture gradient in the center of the product are zero,

$$\frac{\partial T}{\partial r} = \frac{\partial u}{\partial r} = 0 \tag{3.15}$$

The boundary conditions for the surface and the center of the product are summarized in Table 3.1.
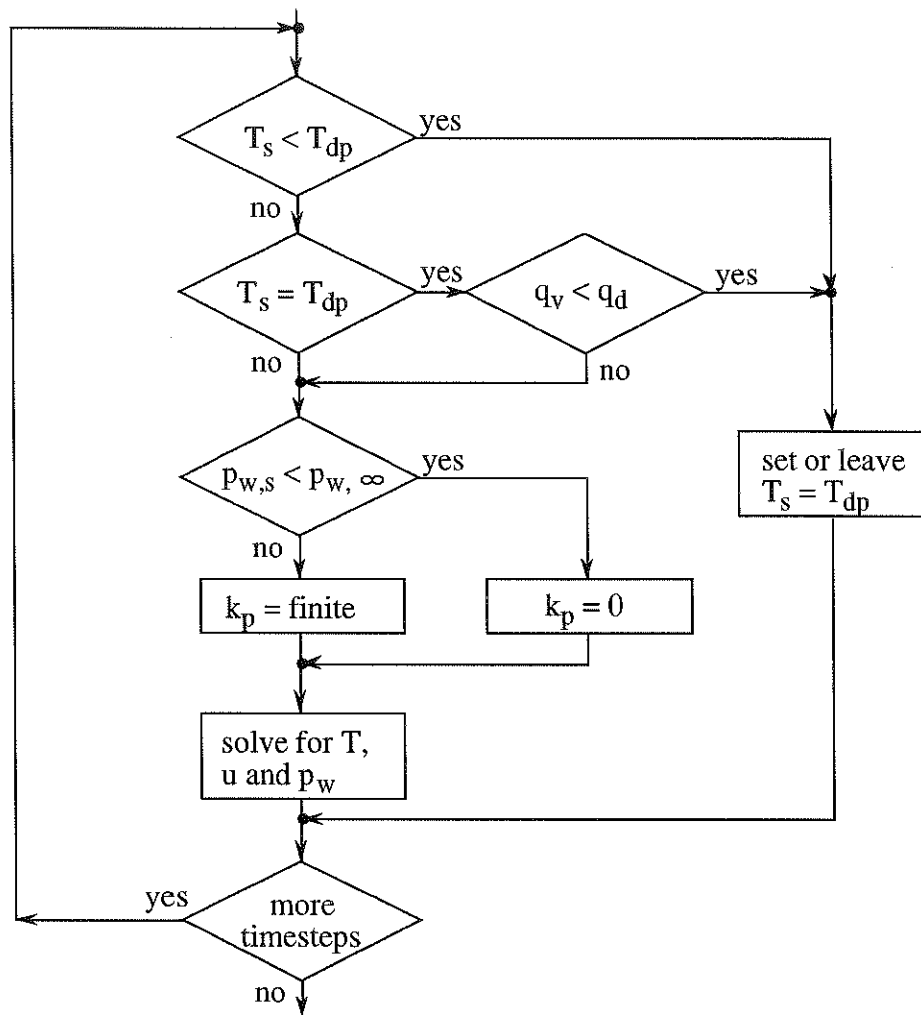
Figure 3.1:   Flowchart of the boundary conditions of the simulation model that do not

allow mass transfer from the process air towards the product during the

condensation period as reported by Schaefer [1995].

24

Table 3.1: Summary of the equations to describe the simulation model.

Conservation Equation
Heat Transfer
$\bar{\rho}\,\bar{c}\,\dfrac{\partial T}{\partial \tau} \;=\; \dfrac{1}{r}\dfrac{\partial}{\partial r}\left(r\,k\,\dfrac{\partial T}{\partial r} + r\,c_w\,\rho_d\,T\,D_{eff}\,\dfrac{\partial u}{\partial r}\right)$
Mass Transfer
$\dfrac{\partial u}{\partial \tau} \;=\; \dfrac{1}{r}\dfrac{\partial}{\partial r}\left(r\,D_{eff}\,\dfrac{\partial u}{\partial r}\right)$

Boundary Conditions at the Surface ($r = R$)	
$T_s = T_{dp}$ $k_p = 0$	if $h\left(T_\infty - T_s\right) < -k\left.\dfrac{\partial T}{\partial r}\right|_s$
$k\dfrac{\partial T}{\partial r} = h\left(T_\infty - T_s\right)$ $k_p = 0$	if $T_\infty > T_s$ and $p_{w,s} < p_{w,\infty}$
$u_s = \displaystyle\sum_{i=1}^{5} a(i)\,RH^i$ $-k\dfrac{\partial T}{\partial r} = h\left(T_\infty - T_s\right) - \Delta\hat{H}_\upsilon\,k_p\left(p_{w,s} - p_{w,\infty}\right)$ $-\rho_d\,D_{eff}\dfrac{\partial u}{\partial r} = k_p\left(p_{w,s} - p_{w,\infty}\right)$	if $T_\infty < T_s$ and $p_{w,s} > p_{w,\infty}$ or for the case where mass transfer to the product is allowed.

Boundary Conditions at the Center ($r = 0$)
$\dfrac{\partial T}{\partial r} = \dfrac{\partial u}{\partial r} = 0$

CHAPTER FOUR

FINITE DIFFERENCE ANALYSIS

The equations derived in the previous chapter describe the total heat and mass transfer of the model. It is not possible to solve these equations analytical for the *** a meat product undergoes, and so the partial differential equations are approximated by finite differences. The derivation of the finite difference model is the subject of this section.

4.1 Approximation of the Differential Equations

There are different possibilities to approximate derivatives. In this work spatial derivatives with second order accuracy will be used. The model is assumed to be a one-dimensional heat and mass transfer problem in a cylindrical product. The product is broken into a finite number of nodes as shown in Figure 4.1.

There are different ways to set the coordinates. One can use constant distances Δr or one can use constant node volumes ΔV. The letter is normally used for rectangular models, former is used for cylindrical models. The center of a node is the location, where the values of the temperature and the moisture content are calculated, it is defined to be in the volumetric center and not in the center between the two surfaces of each node. Thus the temperature of the surface and the center of the model are of most interest, the grid is oriented so that the centers of the first and the last nodes are at the center and at the surface of the cylindrical product. Due to this orientation the surface and the center node will have
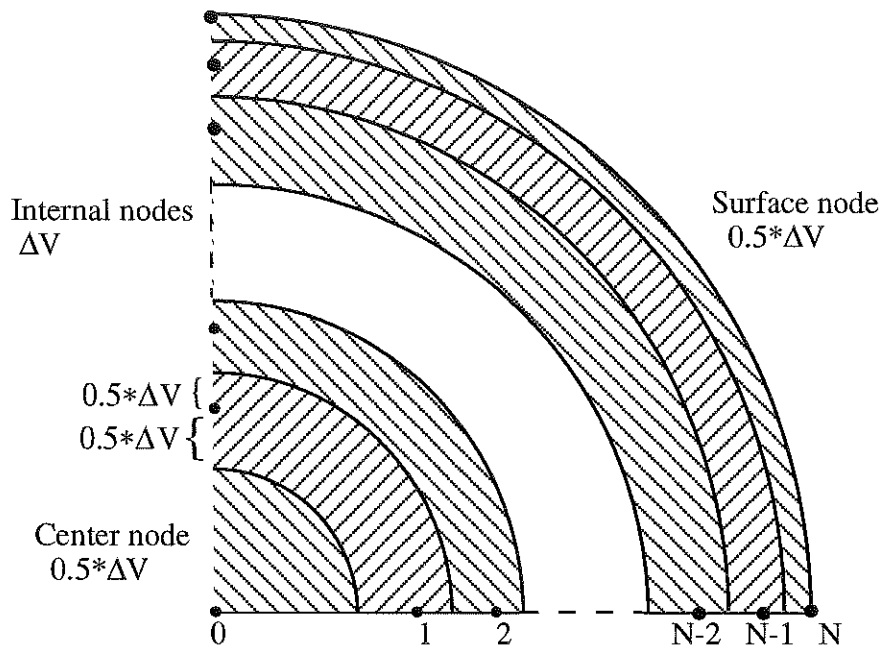
Figure 4.1: Finite difference element presentation of a cylindrical product.

half the volume of the internal nodes of model. The center of the nodes are calculated with equation

$$r(i) \;=\; R\sqrt{\frac{i}{N}} \qquad for\ i = 0,1,2,..,N \tag{4.1}$$

where R is the radius of the product, N the total number of nodes and i the node number. The constant volume of each node can be calculated with equation

$$\Delta V \;=\; \frac{\pi\,R^2\,L}{N} \tag{4.2}$$

where L is the length of the cylinder. These statements are used for the following approximations.

For first order differential equation one can use the forward difference approximation

$$\frac{\partial y}{\partial \tau} = \frac{y_i^p - y_i^{p+1}}{\Delta \tau} + O(\Delta \tau) \tag{4.3}$$

$$\frac{\partial y}{\partial r} = \frac{y_i^p - y_{i+1}^p}{\Delta r} + O(\Delta r) \tag{4.4}$$

or the central difference approximation, that is more accurate, for first and second order differential equations.

$$\frac{\partial y}{\partial r} = \frac{y_{i-1}^p - y_{i+1}^p}{2\Delta r} + O(\Delta r)^2 \tag{4.5}$$

$$\frac{\partial^2 y}{\partial r^2} = \frac{y_{i-1}^p - 2\,y_i^p - y_{i+1}^p}{(\Delta r)^2} + O(\Delta r)^2 \tag{4.6}$$

where i is the number of the node and p is the time step of the calculation. y can either be the temperature T or the moisture concentration u. One can use the explicit or the implicit method for the calculation of the temperature and the moisture concentration. The explicit method uses only known values of previous time steps. The implicit method uses only values of the current time step. The explicit method tents to overpredict the exact solution, while the implicit method tents to underpredict the exact solution. In this work the implicit method is used. So p in the equations 4.4 to 4.6 has to be changed to $p+1$.

4.2 Final Finite Differential Equations

The approximated equations introduced in the previous paragraph are now substituted in the partial differential equation that are listed in Table 3.1. One has to look separately at the center node, the surface node and the internal nodes.

The center node and the surface node represents the boundary conditions of the differential equation that describes the internal nodes. The special cases for the boundary conditions, when the surface temperature is equal to the dew point temperature or when the mass transfer coefficient is assumed to be zero, has to be done with a procedure as shown in Figure 3.1.

The Center Node

$$\frac{\Delta V}{2} \frac{u_0^{p+1} - u_0^{p}}{\Delta \tau} = A_{0.5} D_{eff} \frac{u_1^{p+1} - u_0^{p+1}}{\Delta r}$$

$$\frac{\Delta V}{2} \bar{\rho} \, \bar{c} \frac{T_0^{p+1} - T_0^{p}}{\Delta \tau} = A_{0.5} k \frac{T_1^{p+1} - T_0^{p+1}}{\Delta r}$$

The Surface Node

$$\bar{\rho} \, \bar{c} \frac{\Delta V}{2} \frac{T_N^{p+1} - T_N^{p}}{\Delta \tau} = -A_{(N-0.5)} k \frac{T_N^{p+1} - T_{N-1}^{p+1}}{\Delta r} + A_s \, h \left(T_\infty - T_s\right) - A_s \, \Delta \hat{H}_v \, k_p \left(p_{w,s} - p_{w,\infty}\right)$$

$$\rho_d \frac{\Delta V}{2} \frac{u_N^{p+1} - u_N^{p}}{\Delta \tau} = -A_{(N-0.5)} \rho_d \, D_{eff} \frac{u_N^{p+1} - u_{N-1}^{p+1}}{\Delta r} - A_s \, k_p \left(p_{w,s} - p_{w,\infty}\right)$$

The Internal Nodes

$$\Delta V \frac{u_i^{p+1} - u_i^{p}}{\Delta \tau} = A_{(i-0.5)} D_{eff} \frac{u_{i-1}^{p+1} - u_i^{p+1}}{\Delta r} - A_{(i+0.5)} D_{eff} \frac{u_i^{p+1} - u_{i+1}^{p+1}}{\Delta r}$$

$$\Delta V \bar{\rho} \, \bar{c} \frac{T_i^{p+1} - T_i^{p}}{\Delta \tau} = A_{(i-0.5)} k \frac{T_{i-1}^{p+1} - T_i^{p+1}}{\Delta r} - A_{(i+0.5)} k \frac{T_i^{p+1} - T_{i+1}^{p+1}}{\Delta r}$$

$$+ A_{(i-0.5)} c_w \, \rho_d \, T \, D_{eff} \frac{u_{i-1}^{p+1} - u_i^{p+1}}{\Delta r} - A_{(i+0.5)} c_w \, \rho_d \, T \, D_{eff} \frac{u_i^{p+1} - u_{i+1}^{p+1}}{\Delta r}$$

CHAPTER FIVE

IMPACT OF THE PARAMETERS AND VARIABLES

This chapter introduces the character of the parameters that influence the process simulation and describes the impact of each parameter on the process. One can divide the parameters of the simulation of the thermal meat emulsion process into three groups: *process parameter* , *property data* and *model parameter*. As visualized in Figure 5.1.

Property data

Process parameter → | Model parameter | → T = f (time) u = f (time)
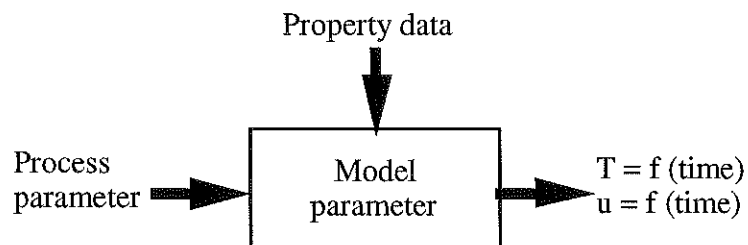
Figure 5.1: Parameter Model with the temperature and the moisture content as output data.

Each group will be introduced and analyzed to get a better understanding of the process. According to the parameter range it will be discussed if a constant value or a parameter model should be used for the simulation of the process, and if the parameters have a higher impact in the beginning or the end of the process. Looking at the impact of one parameter all other parameters are hold at a constant "standard" value. They are listed and marked in Table 5.2.

5.1 Process Parameters

Process parameters are those parameters that can be adjusted with the smokehouse equipment. They can be measured and are well known:

- Temperature T
- Relative Humidity RH
- Air Velocity v
- Time t

and the pressure p , that is assumed to be constant p = 1atm. These parameters have an impact on the heat and mass transfer coefficients at the surface of the product, h and k_p . The equilibrium of the product with the temperature T and the relative humidity RH of the process air gives the physical limit for the heat and mass transfer. They are proportional to the driving forces but their impact on the heat and mass transfer coefficients are very small. The heat and mass transfer coefficients are primarily a function of the air velocity in the smokehouse

5.1.1 Temperature

The definition of "cooking" is a temperature of 68.3°C (155°F) in the center of the product. The higher the temperature of the process air, the higher is the driving force for heat transfer. But the temperature of the surface is limited to avoid product damage, the process air temperature of the smokehouse discussed in this work is limited to about 80°C. Newer smokehouse processes reach temperatures of up to 120°C. The temperature in the center of the product is then about 80°C to reach the same preservation effect as before in a shorter time period. Nevertheless, the temperature doesn't change in a wide range, during the cooking process in the different zones.

5.1.2 Relative Humidity

The relative humidity has a high impact on the process as shown in <u>Figure 5.2</u>, thus the surface temperature in the beginning of the process is assumed to be the dew point temperature of the process air. Assuming the dry bulb temperature to be constant, the surface temperature in the beginning of the process is the higher, the higher the relative humidity RH.
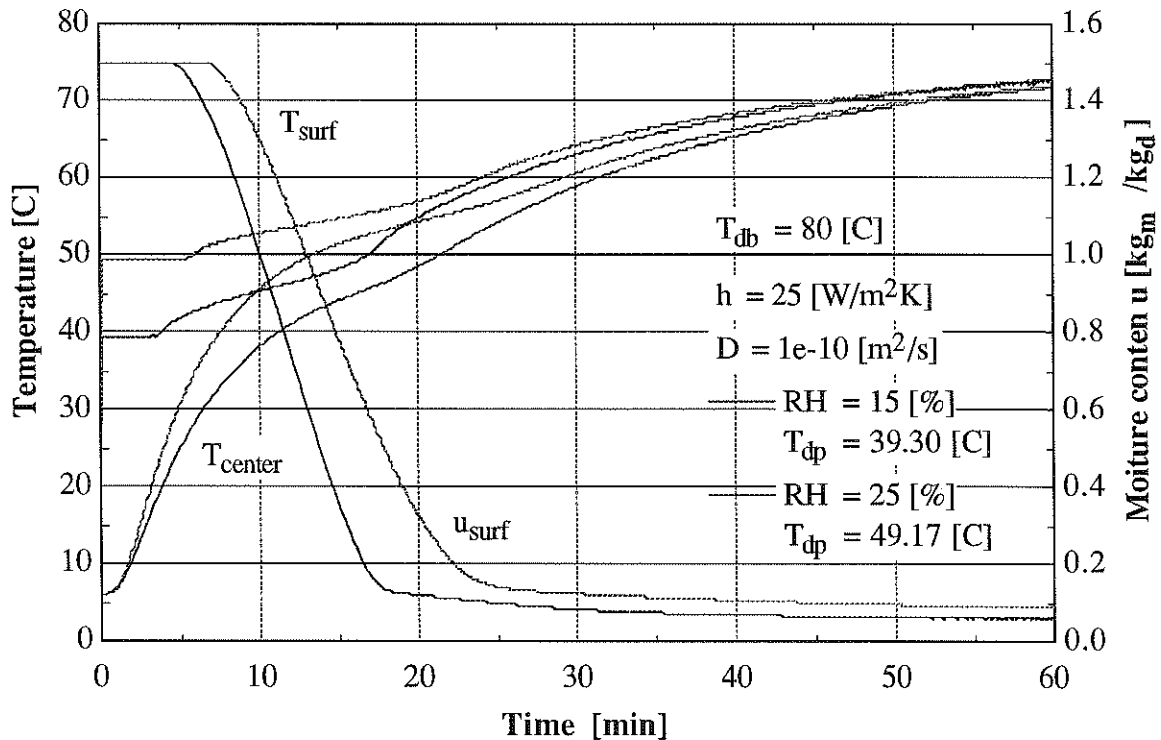
<u>Figure 5.2</u>: Calculated temperature and moisture concentration at the surface and the center of the product for different relative humidities RH.

This leads to a steeper temperature gradient between the surface and the center of the product but a smaller temperature gradient between the surface and the process air. As a

result of the steeper temperature gradient in the inside of the product the temperature of the center will increase more rapidly for higher relative humidities. Thus the product will reach a homogeneous temperature sooner. On the other hand the higher relative humidity will increase the partial vapor pressure in the process air and decrease the driving force for mass transfer at the surface of the product. The mass transfer will start later, because a higher evaporation pressure and a higher surface temperature is needed. Due to the smaller driving force it takes longer to dry the surface to the equilibrium moisture content as shown in Figure 5.2. According to the equilibrium isotherms discussed in Chapter 2 for relative humidities higher than about 70% the mass transfer will be negligible because the equilibrium moisture contents of full fat products is almost equal or higher than the initial moisture content (u_{ini} = 1.5).

Taking all this into account, the surface temperature of the product in the end of the mass transfer process is almost the same for relative humidities of 15 and 25 %. The end of the drying process is indicated by a constant equilibrium surface moisture content of about 0.1 kg_m/kg_d. Figure 5.3 shows the moisture ratio as a function of time. m_0 is the initial moisture content and m is the current moisture content. Consistent with Figure 5.2 it shows that the mass transfer starts later for higher relative humidities. One can also see that after the drying process of the surface the moisture ratio is very similar for different relative humidities. Thus the lower moisture loss of 6.7% (RH = 25%) for higher relative humidities is both a reason of the higher vapor pressure of the process air and the faster temperature rise to 68.3°C of the center of the product.
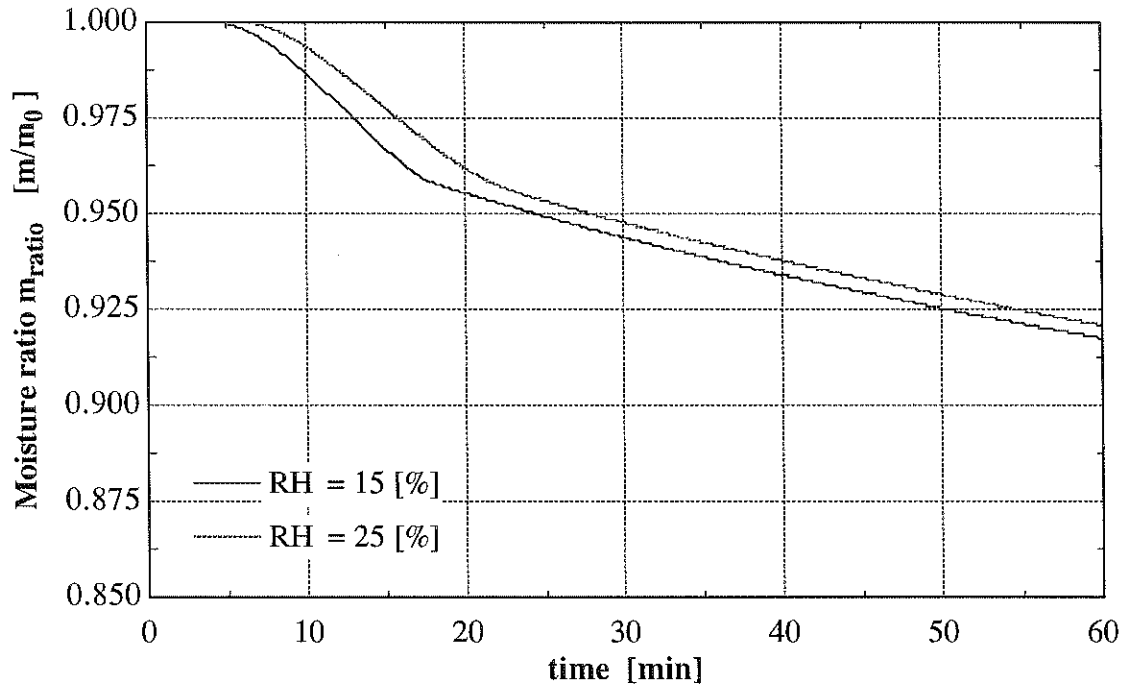
Figure 5.3: Impact of the relative humidity RH on the moisture ratio m/m_0.

So changes of the relative humidity between 10% and 60% will change the performance in the beginning of the process, while after a longer time period the product conditions are essentially the same.

5.1.3 Air Velocity and Heat Transfer Coefficient

The air velocity above the surface of the product has a high impact on the heat and mass transfer coefficient. To calculate the actual heat and mass transfer coefficients the air velocity and the flow pattern must be known. The air velocity can be calculated with the size of the smokehouse and the air volume traveling through the different zones. The flow pattern may be simplified to "flow over a flat plate" or "cylinder in cross flow". Spielbauer [1993] measured the heat transfer coefficient and showed that neither of these simplified models gives a good result. The measured average data of each zone vary in a wide range

from 17 to 31 W/m²K and Spielbauer suggests the average value of the heat transfer coefficients calculated with these to methods. He also measured significant variation of the heat transfer coefficient at the top and the bottom of the zones as a result of the different flow patterns. This work is based on the assumption that the heat transfer coefficient is constant in each zone. The calculation of the heat transfer coefficient as a function of the air velocity needs further investigations, thus in this work the impact of the air velocity is discussed in terms of the impact of the heat transfer coefficient. Knowing the heat transfer coefficient, the mass transfer coefficient can be calculated with the Equations 5.1 to 5.4:

$$\frac{h}{k_{x,m}} = \tilde{c}_{p,f} \left(\frac{\alpha}{D_{AB}} \right)^{2/3} \tag{5.1}$$

where the mass transfer coefficient $k_{x,m}$ is based on a mole fraction driving force and $\tilde{c}_{p,f}$ is the specific heat of moist in air. α is the heat diffusivity and D_{AB} is the mass diffusivity of moisture in air. The specific heat as a function of the relative humidity RH in J/mol-K for a pressure of p = 1 atm and a temperature of 80°C can be calculated with

$$\tilde{c}_{p,f} = 29.0 + 15.6 * RH + 0.987 * RH^2 + 10.0 * RH^3 \tag{5.2}$$

The mass diffusivity in m²/s of moisture in air can be calculated with

$$D_{air,water} = 0.28 10^{-4} \left(\frac{T[K]}{298} \right)^{3/2} \tag{5.3}$$

To obtain a mass transfer coefficient based on a vapor pressure driving force k_p, the coefficient $k_{x,m}$ can be converted with the relation

$$k_p = k_{x,m} \frac{M_w}{P_t} \tag{5.4}$$

where M_w and P_t are the molecular weight of water and the total pressure, respectively.

The impact of the heat and mass transfer coefficients on the thermal process is shown in Figure 5.4 and 5.5. For each zone the coefficients are assumed to be constant and do not vary independent of each other. They are not treated separately, because the variation of the mass transfer coefficient is very small and the impact on the process negligible as shown by Schaefer [1996].

Figure 5.4 shows the temperature and the moisture concentration at the surface and center of the product for heat transfer coefficients of h = 25 W/m^{2}K (kp = 1.47e-4 kg/Pa m^{2}s) and h = 30 W/m^{2}K (kp = 1.74e-10 kg/Pa m^{2}s). It can be seen that the variation of the heat and mass transfer coefficients has only a small impact in the beginning of the process and a large impact at the end. The small impact in the beginning is due to the assumption that the surface temperature is equal to the dew point temperature, which is not a function of these transfer coefficients. In the beginning of the mass transfer process the effect of a higher heat and mass transfer coefficient on the surface temperature cancel each other out. A higher heat transfer coefficient increases the heat transfer rate to the surface. A higher mass transfer coefficient increases the mass transfer rate towards the surface thus

36
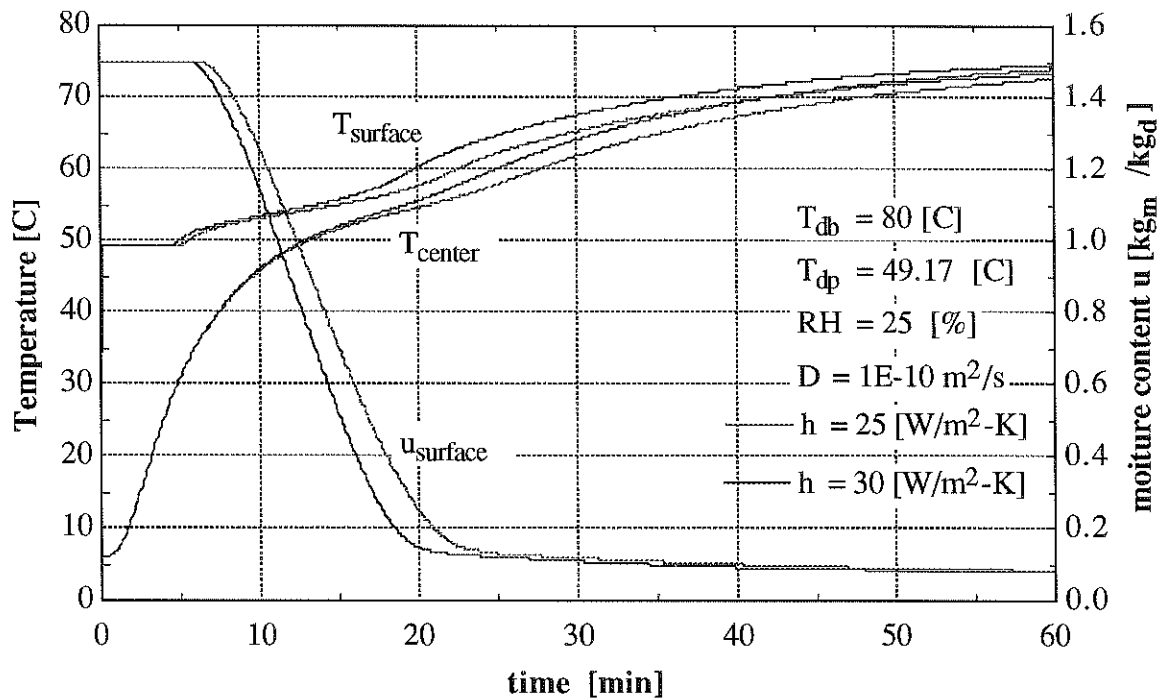
Figure 5.4:   Calculated temperature and moisture concentration at the surface and center of the product.

increasing the heat loss at the surface due to evaporation. This causes the surface to dry faster for higher heat and mass transfer coefficients. As long as the higher mass transfer rate compensates for the higher heat transfer rate, the impact of a higher heat transfer coefficient on the surface temperature will be rather low. As soon as the mass transfer rate decreases the higher heat transfer will increase the rate at which the product temperature rises and so decrease the cooking time. Figure 5.5 shows that for higher heat and mass transfer coefficients the moisture ratio will decrease quicker in the beginning of the mass transfer process. When the surface reaches the equilibrium moisture concentration the curve for h = 25 W/m²K and h = 30 W/m²K are practically the same. Before the equilibrium moisture content is reached a steeper gradient is shown by both processes.
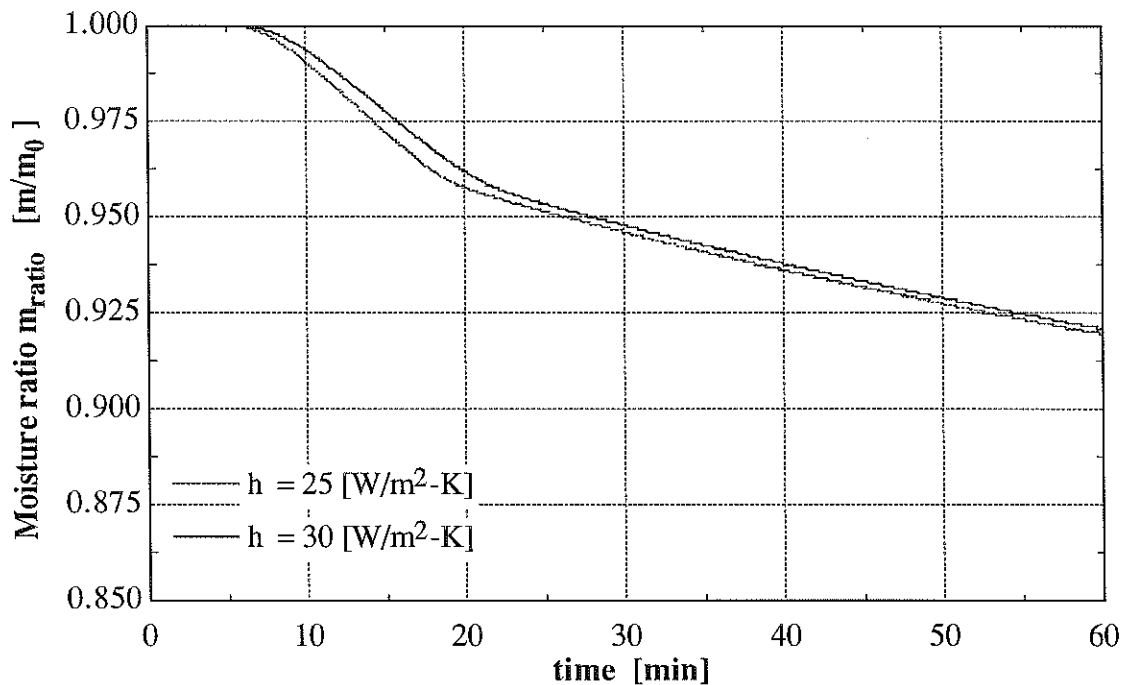
Figure 5.5: Moisture ratio as a function of time for heat transfer coefficient of h = 25/30 W/m²K.

5.2 Property Data

Each meat emulsion sample has slightly different property data. They vary for the same emulsion compositions due to different meat quality and with different kinds of mixtures, like full-fat and non-fat emulsions. The following property data will be discussed in this work:

- Effective Moisture Diffusivity D_{eff}

- Heat conductivity k

- Density ρ

- Specific Heat c

The property data will also vary with temperature and moisture content, as discussed in Chapter 2. The process parameters primarily influence the heat and mass transfer

coefficients at the surface. The property data primarily influence the heat and mass transfer coefficients inside the product. This chapter will discuss some models that describe the property data as a function of temperature and moisture content. The range of the variation of the property data will than be compared with the impact of these property data on the process. For small property changes and low impacts on the process, properties will be assumed to be constant.

5.2.1 Effective Moisture Diffusivity

The effective moisture diffusivity inside the product has the strongest impact of the process. It does not change the process in the beginning as shown in Figure 5.6. But in the end of the process the impact of the effective moisture diffusivity is significant due to the larger moisture transfer from the inside to the surface of the product. Thus more moisture diffuses to the surface and evaporates, the evaporation heat losses will increase and less energy is available to rise the product temperature. The moisture loss for $D = 1E\text{-}10 \ m^2/s$ is $m_{loss} = 6.7\%$ with a cooking time of $t_{cooking} = 45.7$ min and for $D = 5E\text{-}10 \ m^2/s$ is $m_{loss} = 35\%$ with a cooking time of $t_{cooking} = 155$ min. The higher moisture diffusivity rate is indicated in Figure 5.7 by a steeper gradient of the moisture ratio. When the surface reached the equilibrium moisture content, the gradient is constant. Because the mass transfer process is diffusion limited, the mass transfer rate is proportional to the moisture diffusivity coefficient. A higher moisture diffusivity causes a higher mass loss as shown in Figure 5.7.
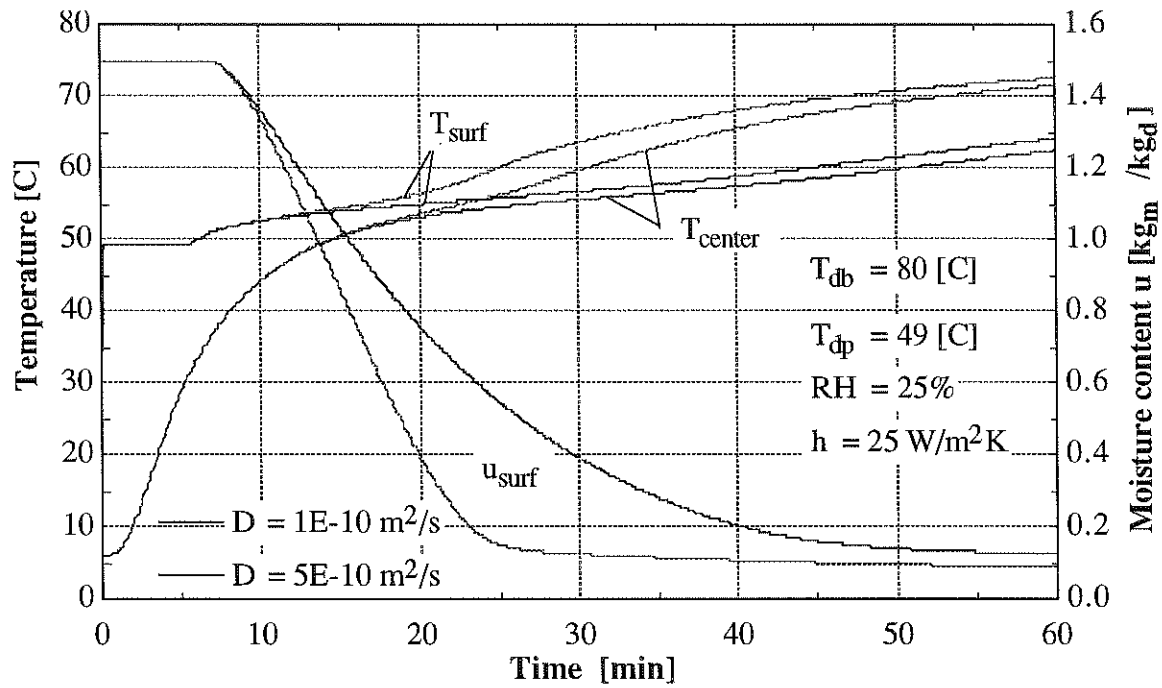
Figure 5.6: Calculated temperature and moisture concentration at the surface and center of the product for different effective moisture diffusivities.
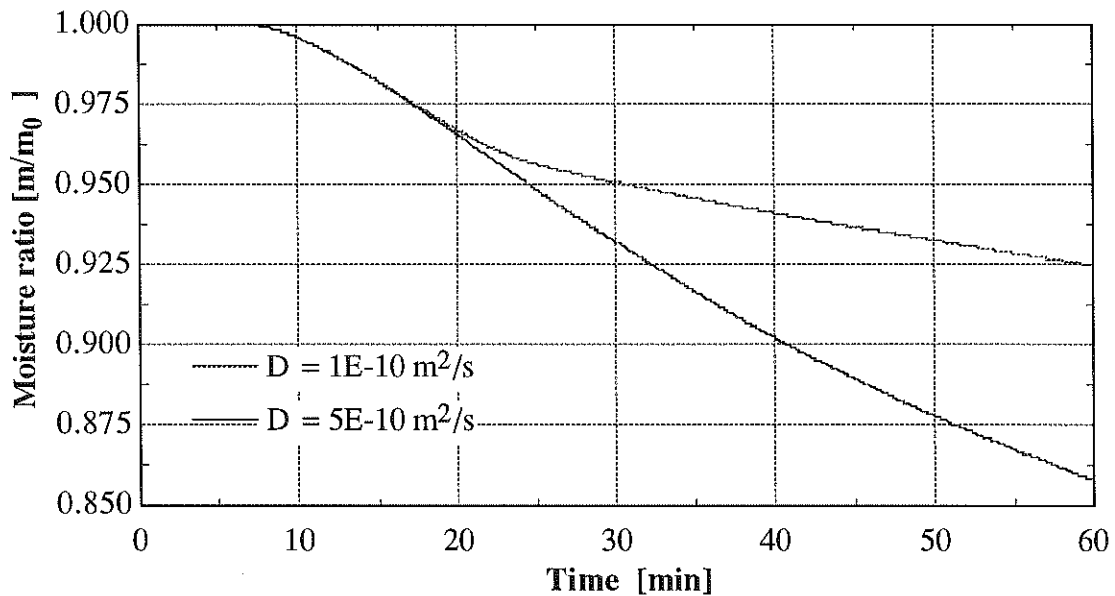
Figure 5.7: Moisture ratio as a function of time for effective moisture diffusivity coefficients of Deff = 1E-10 and 5E-10m²/s.

The larger evaporation heat losses increase the "cooking" time. The moisture loss and the cooking time will increase rapidly for higher moisture diffusivity coefficients. Recalling the variable range of the moisture diffusivity of several magnitudes as introduced in Chapter 2, it is obvious that a model for the moisture diffusivity coefficient has to be chosen very carefully. Figure 5.8 shows the moisture concentration profile of the product.
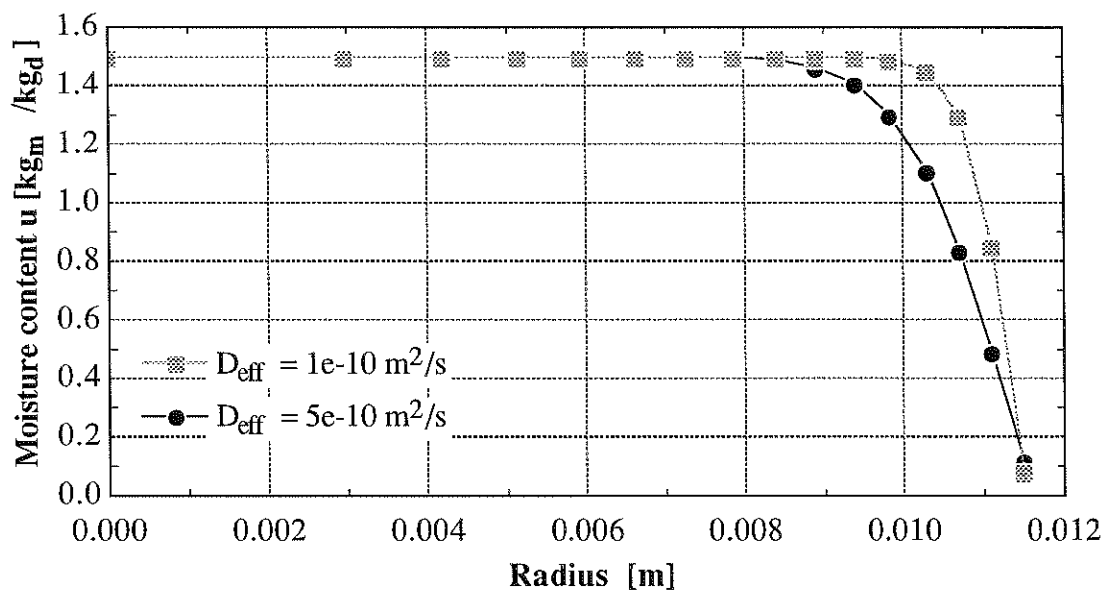
Figure 5.8: Moisture profile of cylindrical product for different moisture diffusivities.

The larger the moisture diffusivity, the smaller the moisture gradient at the surface of the product and the deeper the penetration depth of the drying process. The temperature difference between center and surface decreases also faster for larger moisture diffusivities.

5.2.2 The Conductivity

Different models are available for the conductivity of the meat emulsion as listed in Table 2.1 . Constant values are given for different moisture concentrations an temperatures

as well as the conductivity as a function of the moisture content. The values vary in a range of $k = 0.355$ W/m^{2}K to $k = 0.576$ W/m^{2}K for wet-weight moisture concentrations of $\omega_m = 0.54$ to 0.80 kg$_m$/kg ($u_m = 1.17$ to 4.0 kg$_m$/kg$_d$). The model of Swaet [1975] is based on a wet-weight moisture concentration range of $\omega_m = 0.60$ to 0.80 kg$_m$/kg ($u_m = 1.5$ to 4.0 kg$_m$/kg$_d$). The initial moisture content of full-fat products discussed in this work is $u_{m,ini} = 1.5$ kg$_m$/kg$_d$ for the simulations in this chapter and $u_{m,ini} = 1.359$ kg$_m$/kg$_d$ for the process simulation in Chapter 6. Thus using the model of Swaet [1975] will give an almost constant value for full-fat products. For non-fat products with an initial dry-weight moisture content of $u_{m,ini} = 6.69$ kg$_m$/kg$_d$ it will have a more significant impact. According to the range of the model of Swaet [1975] Figure 5.9 shows the impact of the conductivity of $k = 0.4$ W/m^{2}K and $k = 0.5$ W/m^{2}K.

$T_{db} = 80$ [C]

$T_{dp} = 49.17$ [C]

RH $= 25$ [%]

$D = 1E\text{-}10$ m^2/s

h $= 25$ [W/m^2-K]

-------- k $= 0.4$ W/m^2 K : $t_{cooking}$ $= 45.5$ min   moisture loss $= 6.6\%$

-------- k $= 0.5$ W/m^2 K : $t_{cooking}$ $= 43.1$ min   moisture loss $= 6.5\%$
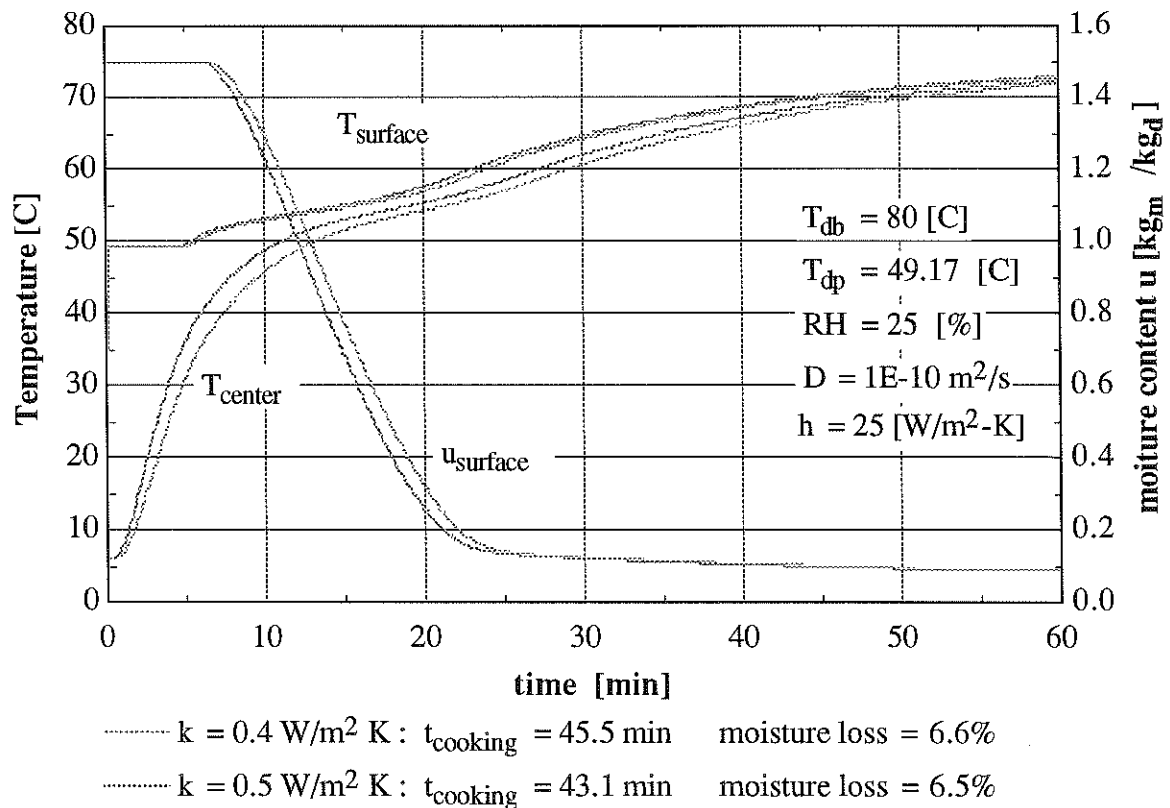
Figure 5.9:   Calculated temperature and moisture concentration at the surface and center of the product for different conductivities.

Increasing the conductivity from 0.4 W/m^{2}K to 0.5 W/m^{2}K decreases the cooking time from $t_{cooking}$ = 45.5 min to $t_{cooking}$ = 43.1 min. It is important to see that the larger impact of the higher conductivity is limited to the center of the product that rises faster and so decreases the cooking time. The product is heated more homogeneous. The impact of the higher conductivity on the mass transfer process is less significant. Even though the surface temperature dries faster in the beginning, the time needed to reach the equilibrium
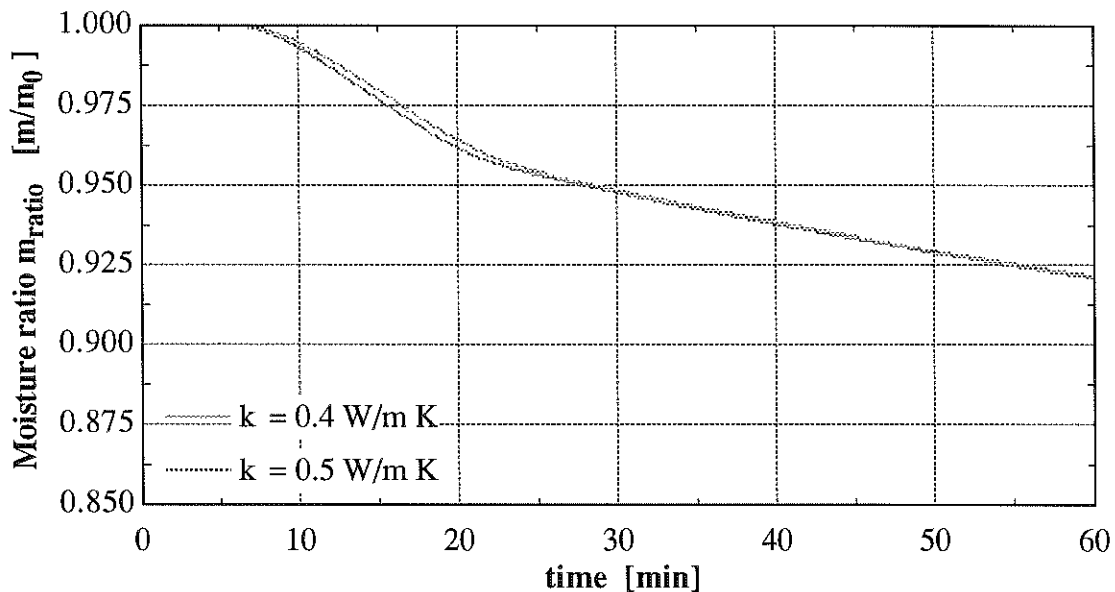
Figure 5.10: Moisture ratio as a function of time for conductivities k = 0.4 W/m^{2}K and k = 0.5 W/m^{2}K

moisture content is almost the same. As shown in Figure 5.10 the moisture ratio profile is practical the same, and so is the moisture loss of 6.6% for k = 0.4 W/m^{2}K and 6.5% for k = 0.5 W/m^{2}K.

In the process simulation model the conductivity model of Swaet [1975] is used, that is identical to k = 0.4 W/m^{2}K for the simulations discussed in this chapter thus the lower limit of this model is k = 0.392 W/m^{2}K for dry-weight moisture contents below u = 1.5kg$_m$/kg$_d$.

5.2.3 The Density

The density of the meat emulsion is reported to be about $\rho = 1000$ kg/m^3 as listed in Table 3.1. It is more the change of the composition than the change of the total density that one has to look at. The total density is calculated with $\rho = \rho_m + \rho_d$ where ρ_m and ρ_d are the moisture density and the dry density as discussed in Chapter 3. The composition changes when the moisture content of a meat emulsion changes like for full-fat, low-fat and non-fat meat emulsions. Changes of the composition have a significant impact of the moisture diffusivity of the meat emulsion, for a better understanding of the complex process the moisture diffusivity is assumed to be constant for this simulation. The measured data given by Schaefer [1995] for a full-fat and a non-fat meat emulsion are listed in Table 5.1.

Table 5.1:   Results from the determination of the dry density of full-fat and no-fat meat emulsions based on the total density and the moisture content.

Sample	Mass [g]	Volume [ml]	Total density [kg$_t$/m^3]	Wet-moisture content [kg$_m$/kg$_t$]	Dry-moisture content [kg$_m$/kg$_d$]	Dry density [kg$_d$/m^3]
full-fat product	119.8	117	1024	0.576	1.358	434
non-fat product	138.8	134	1036	0.870	6.692	135

Figure 5.11 shows the impact of different moisture contents comparing the same process for a full-fat and a non-fat product with the values given in Table 5.1. The temperature of the surface of the product in the beginning and during the first minutes of mass transfer are almost the same, while the temperature of the center of the product rises faster for the non-fat product with a higher moisture content. Towards the end of the mass

transfer process the temperature of the product is very homogenous. After the mass transfer is finished the temperature difference between center and surface rises again due to the lower evaporation heat loss at the surface. Due to higher moisture content more moisture has to evaporate at the surface. The drying process is only slightly longer, but the effect on the surface temperature is large.
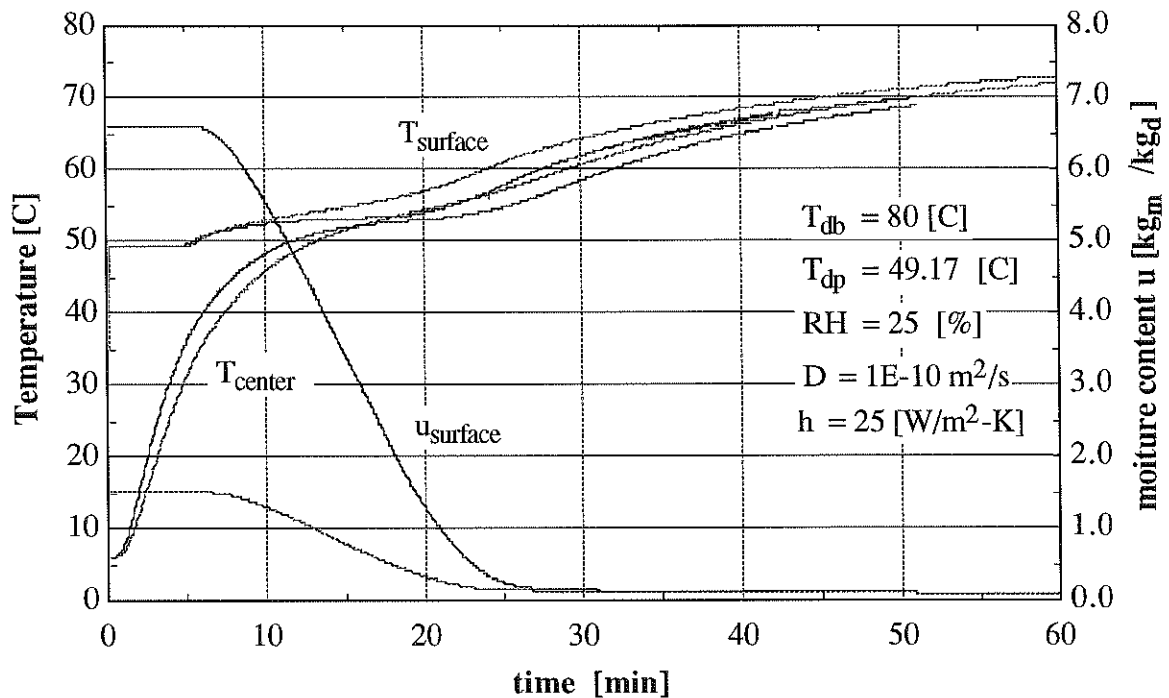
u_{ini} = 1.5 kg_m/kg_d $t_{cooking}$ = 45.5 min   moisture loss = 6.6%
u_{ini} = 6.6 kg_m/kg_d $t_{cooking}$ = 49.3 min   moisture loss = 6.6%

Figure 5.11: Calculated temperature and moisture concentration at the surface and center of the product for different moisture contents.

The higher moisture content will increase the cooking time from tcooking = 45.5 min for the full-fat product to tcooking = 49.3 min for the non-fat product. While the percentage of moisture loss is almost constant 6.6%. The lower moisture ratio rate of the non-fat product
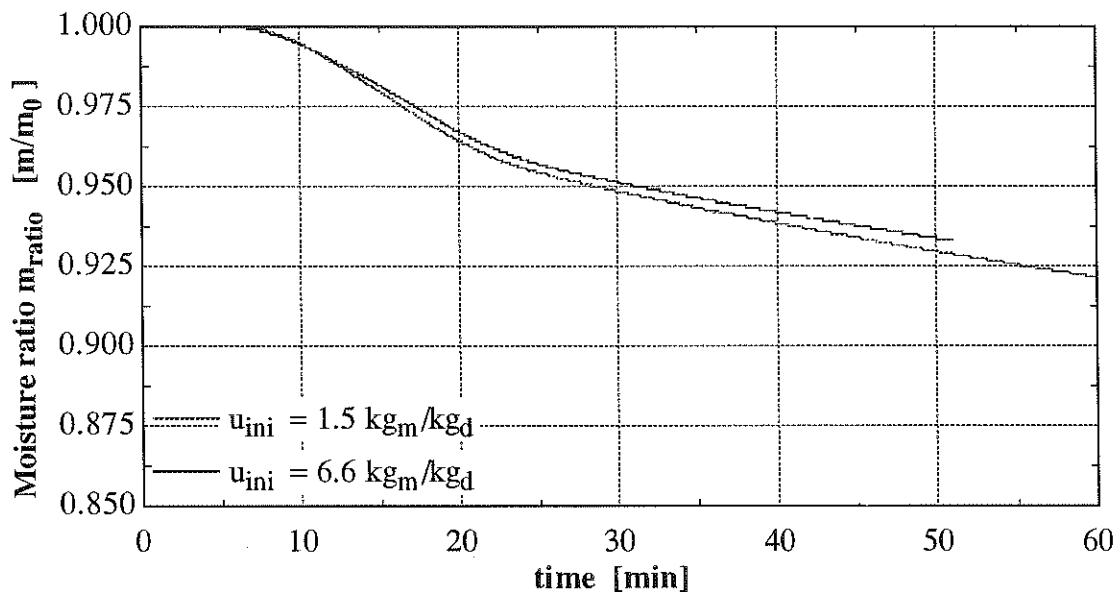
Figure 5.12: Moisture ratio as a function of time for products with different moisture
contents

is compensated by the longer cooking time as shown in Figure 5.12. Nevertheless one has

to take into account that the total mass loss will increase significantly, thus the initial

moisture content of the non-fat product is about 50% higher. But still the moisture

diffusivity and not the moisture content itself is the parameter with the largest impact on the

process. Thus a meat emulsion with a higher moisture content also has a higher moisture

diffusivity, these two effects will add up.

5.2.4 The Specific Heat

The specific heat of the meat emulsion can be calculated with the specific heat of the dry

meat product and the specific heat of the moisture. The specific heat of the dry meat product

c_d is about constant, the specific heat of the moisture c_w can be calculated as a function of

the temperature T [K]. The specific heat of the moist meat product can be calculated with the Equation 5.1 to 5.3:

$$c_d = 1580 \quad [J/kgK] \tag{5.1}$$

$$c_w = \sum_{i=0}^{5} c(i) \cdot T^i \quad [kJ/kg\,K] \tag{5.2}^2$$

$$\bar{c} = \omega_m\,c_w + (1-\omega_m)\,c_d \tag{5.3}$$

where ω_m is the wet moisture concentration. The unit of the specific heat is J/kg K. The range of the specific heat of the moisture is very low (c_w = 4000 to 4130 J/kg K). Due to the drying process the range of the specific heat of the moist meat emulsion is larger ($\bar{c}$ = 1500 to 3600 J/kg K). Thus the specific heat of the moist product changes with the moisture content of the meat emulsion, the specific heat will change during the mass transfer process and stay almost the same before and after the mass transfer process. The impact of the specific heat is shown in Figure 5.13 for a constant specific heat of the moisture of c_w = 4100 J/kg K and to constant values for the specific heat of the moist meat emulsion $\bar{c}$ = 2600 and 3600 J/kg K.

---

[2] $c(0) = 757.1$; $c(1) = -11.56$; $c(2) = 7.0838e-2$; $c(3) = -2.1655e-4$; $c(4) = 3.3019e-7$; $c(5) = -2.0088e-10$

$C_{bar}/C_w = 2600/4100$: $t_{cooking} = 36.0$ min $m_{loss} = 6.1$ %

$C_{bar}/C_w = 3600/4100$: $t_{cooking} = 45.7$ min $m_{loss} = 6.6$ %
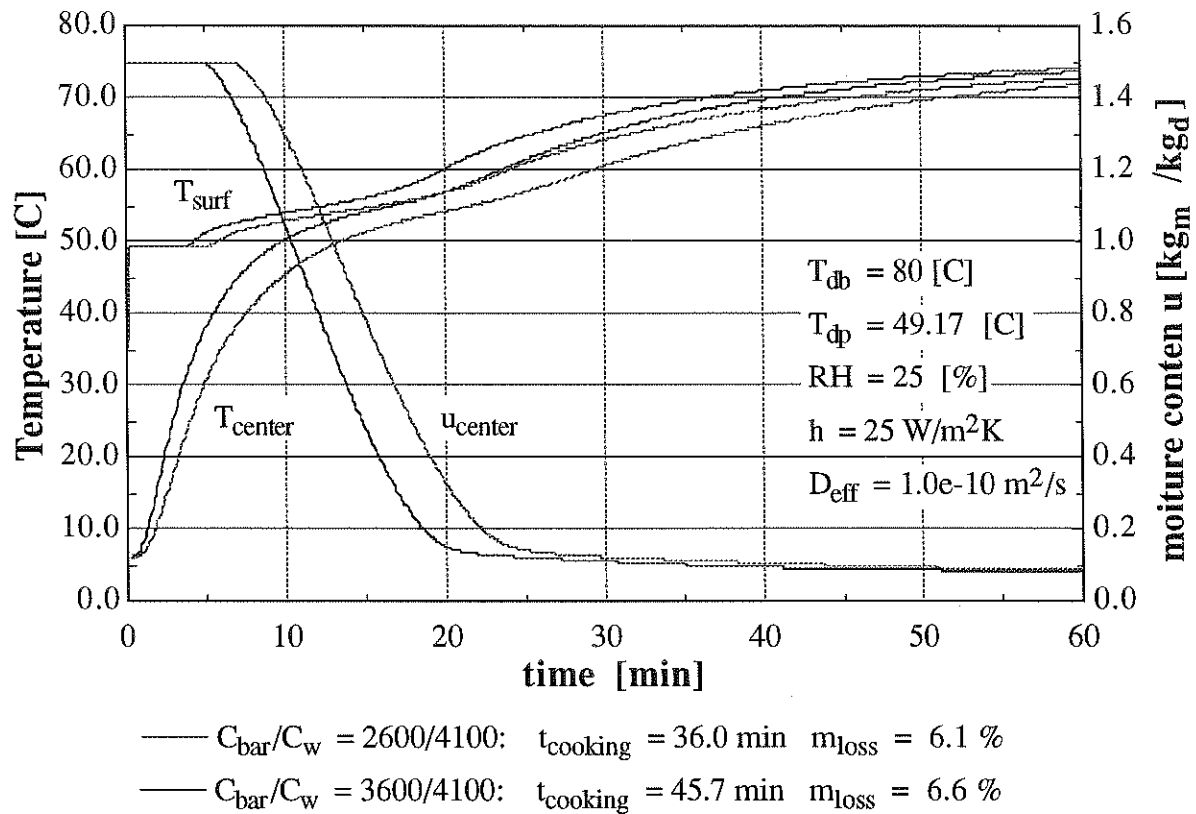
Figure 5.13: Calculated temperature and moisture concentration at the surface and center of the product for different values of the specific heat.

The impact is found to be very significant. Decreasing the specific heat $\bar{c}$ from 2600 J/kg K to and 3600 J/kg K decreases the cooking time from 45.7 min to 36.0 min. The heat load needed to raise the product with the lower specific heat is smaller and the temperatures will rise faster. Thus the mass transfer will start earlier. If the Equations 5.1 to 5.3 are used the temperature profile and moisture content profile will be about the same as for a constant specific heat of $\bar{c}$ = 3100 J/kg K as listed in Table 5.2. The impact on the moisture ratio rate is small as shown in Figure 5.14 and the lower moisture loss for a lower specific heat is a reason of the shorter cooking time.
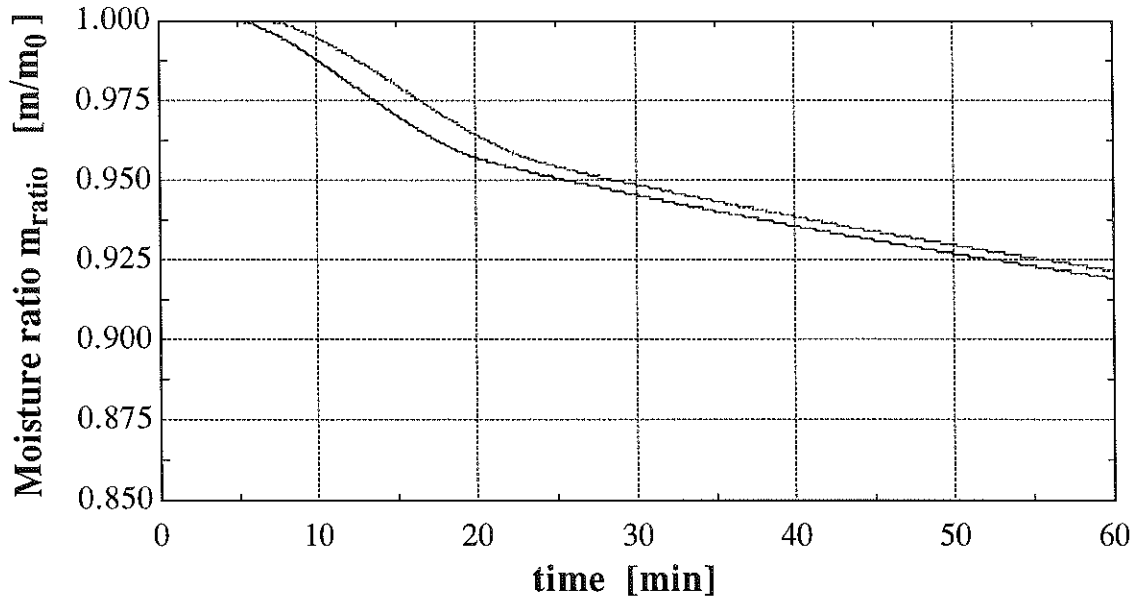
Figure 5.14: Moisture ratio as a function of time for products with different values of the specific heat of the moist product.

For the simulations in this chapter, the specific heat is assumed to be constant. The specific heat of the moisture is set to $c_w = 4100$ J/kg K, the specific heat of the moist meat emulsion is assumed to be $\bar{c} = 3100$ J/kg K.

5.3 Model Parameter

The model parameter of the finite difference model are the number of nodes N and the time step Δt. Even though the implicit differential method is used in this work, there is a critical time step if the variable changes are small. Decreasing the time step below the critical time step still gives the same results as for the critical time step. Changing the number of nodes has a significant impact on the length of the mass transfer process of the simulation model as shown in Figure 5.15 and Figure 5.16
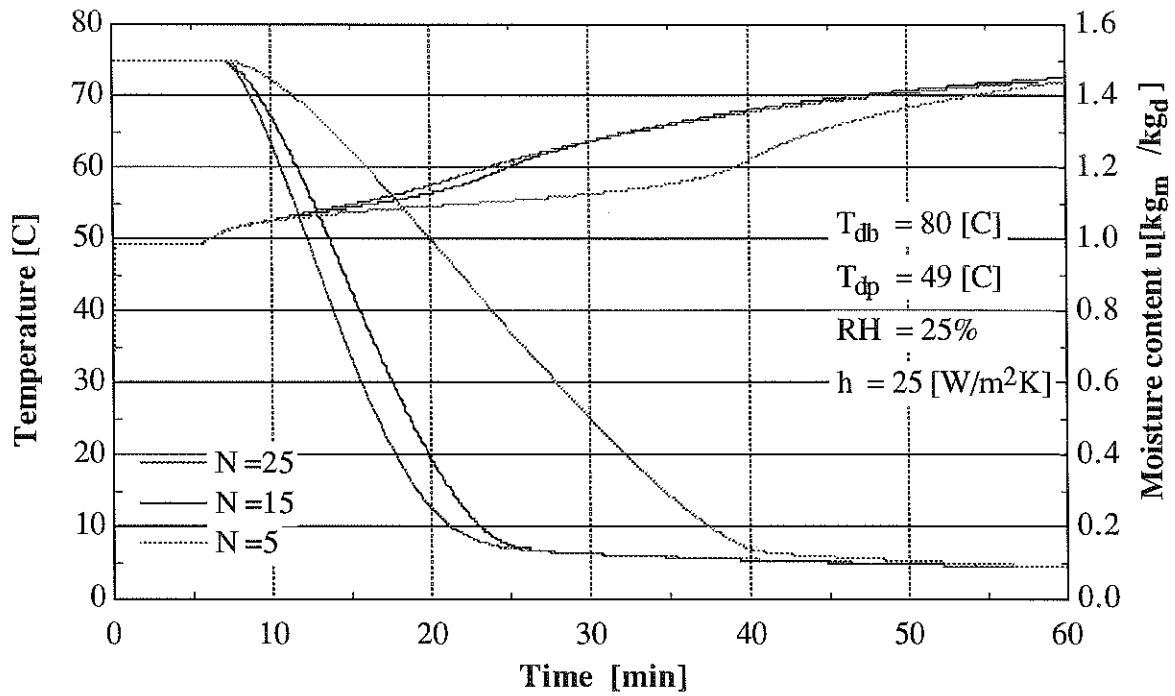
Figure 5.15: Calculated temperature and moisture concentration at the surface and center of the product for different numbers of nodes.
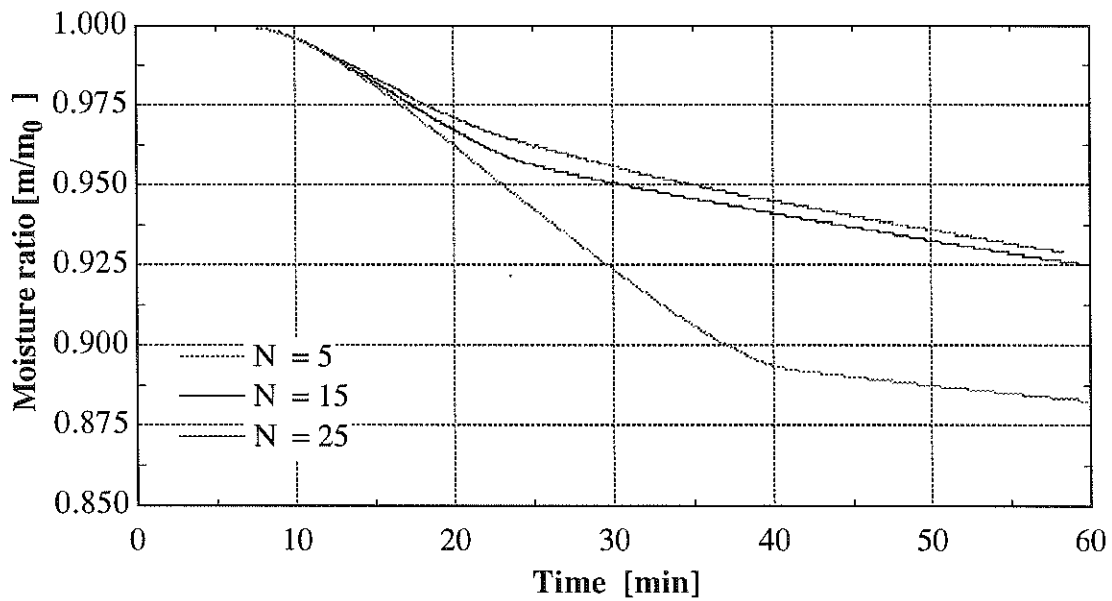
Figure 5.16: Moisture ratio as a function of time for different numbers of nodes.

One can see that the temperature for lower node numbers increases slower than for higher node numbers. It also shows that it takes longer to reach the equilibrium moisture content at the surface. The reason for this significant influence is the equilibrium relationship between the product surface and the process air. The finite difference method sets the moisture content of the whole surface node equal to the equilibrium moisture content. Thus, the higher the volume of the nodes, the higher the moisture loss. The volume of the nodes increases if the node number decreases. Since the surface area stays the same, while the total amount of moisture that needs to evaporate increases, the time needed to reach the equilibrium will increase for smaller node numbers. Due to the higher moisture loss the evaporation heat losses are higher and increase the cooking time. If the number of nodes is increased to infinity, the moisture content of the surface node will instantly drop to the equilibrium moisture content when the mass transfer starts. The slope of the moisture ratio as a function of time as shown in Figure 5.16 would be constant. According to measured data Schaefer [1995] showed that the moisture loss rate is not constant. This rises the question for the optimum number of nodes. For node number over 15 the impact will decrease rapidly, thus in terms of saving computing time the node number of the model in this work is 15.

Table 5.2: Sensitivity of the computer simulation results to different values of the parameters [1]

Input parameter	Units	Value[2]	Cooking time[3] [min]	Moisture loss[4] [%]	Surface temperature[4] [C]	Surface concentration[4] [kg_m/kg_d]
RH	%	7	48.0	7.7	70.2	0.05
		15	47.2	7.2	70.1	0.06
		<u>25</u>	45.7	6.6	70.0	0.10
		50	32.5	3.2	69.1	0.57
		70	13.1	0	72.0	1.5
h	$W/m^2 K$	15	81.1	8.7	69.1	0.10
		20	57.7	7.4	69.6	0.10
		<u>25</u>	45.7	6.6	70.0	0.10
		30	38.33	6.2	70.5	0.10
		50	22.1	5.3	72.8	0.09
D_{eff}	m^2/s	<u>1e-10</u>	45.7	6.6	70.0	0.1
		5e-10	90.0	19.7	69.2	0.4
k	W/mK	<u>f(u)[5]</u>	45.7	6.6	70.0	0.10
		0.4	45.5	6.6	70.0	0.10
		0.5	43.1	6.5	69.7	0.10
ρ/ρ_d	kg/kg_d	<u>1024/434[6]</u>	45.7	6.6	70.0	0.10
		1036/135	49.3	6.6	69.5	0.10
$\bar{c}$ [7]	J/kg K	2600	36.0	6.1	69.9	0.10
		3100	40.9	6.4	70.0	0.10
		f(T,u)/f(u)[8]	40.3	6.3	70.0	0.10
		<u>3600</u>	45.7	6.6	70.0	0.10
N	-	5	54.6	11.6	70.4	0.09
		<u>15</u>	45.7	6.6	70.0	0.10
		25	46.5	6.4	69.9	0.10

[1]process conditions: T_{dp} = 80 C; T_0 = 6 C
[2]the underlined values are used when the other input parameters are varied
[3]time when the center reaches the temperature 68.3C (155F)
[4]values taken at cooking time
[5]model reported by Sweat [1975] Table 2.2
[6]initial moisture content set to u_{ini} = 1.5 kg_m/kg_d
[7]the specific heat of the moisture is constant c_w = 4100 J/kg K if $\bar{c}$ is a constant value
[8]models introduces with Equation 5.1 to 5.3

CHAPTER SIX

PROCESS SIMULATION

The final goal of this work is the simulation of the whole thermal process as described in Chapter 1, and to find ways to improve the process, taking into account the limits due to physical and chemical changes of the product. In this chapter the simulation results are compared to measured data by Spielberg [1992] and Schaefer [1995]. Then it is discussed how the process can be improved to reach processing times of modern smokehouses.

Table 6.1: Values of the model parameters that do not change with simulations of different processing conditions.

Simulation parameter	
heat of evaporation of water [kJ/kg]	$\Delta \hat{H}_v \;=\; 3165 - 2.426\,T\;[K]$
specific heat [kJ/kg][1]	$c_d \;= 1.58$ $\bar{c} \;=\; \omega_d\,c_d \;+\; \omega_w\,c_w$ $c_w \;= \Sigma\, c_i\, T^i \quad , i = 0 - 5$
thermal conductivity [W/m K]	$k \;= 0.080 + 0.52\,\omega_m$
equilibrium moisture content [kg_m/kg_d][2]	$u_s \;=\; \displaystyle\sum_{i=1}^{5} a(i)\, RH^i$

[1]$c_0 = 757.1, c_1 = -11.56, c_2 = 7.0838e-2, c_3 = -2.1655e-4, c_4 = 3.3019e-7, c_5 = -2.0088e-10$
[2]$a_1 = 1.08002, a_2 = -8.3266, a_3 = 30.65, a_4 = -48.919, a_5 = 28.408$

6.1 Reliability of the Simulation Model

To show the reliability of the process simulation, the results of the EES simulation program used in this work are compared to the results of the FORTRAN simulations of Schaefer [1995] and measured data. For the EES Program the constant moisture diffusivity coefficient estimated with a parameter estimation program by Schaefer are used. The measured heat transfer coefficient is $h = 33.3$ W/m^{2}K. The full-fat and no-fat products have a initial moisture content of $u_{ini} = 1.358$ kg$_m$/kg$_d$ and $u_{ini} = 6.692$ kg$_m$/kg$_d$, respectively. The relative humidity and the moisture diffusivity coefficients as estimated by Schaefer are listed in Table 6.2.

Table 6.2: Results of the parameter estimation program used by Schaefer [1995].

Effective moisture diffusivity [m^2/s] as reported by Schaefer [1995] and used in the following work.		
temperature profiles from small diameter products		
	full-fat product	no-fat product
RH = 6.1%	$D_{eff} = 2.24$ e-10	$D_{eff} = 3.55$ e-10
RH = 15.6%	$D_{eff} = 1.07$ e-10	$D_{eff} = 2.52$ e-10
RH = 32.4%	$D_{eff} = 1.13$ e-10	$D_{eff} = 1.77$ e-10
	$D_{eff,avg.} = 1.48$ e-10	$D_{eff,avg.} = 2.61$ e-10
moisture loss experiments		
full-fat product in the laboratory apparatus	$D_{eff} = 0.987$ e-10	
full-fat product in the laboratory apparatus	$D_{eff} = 3.73$ e-10	
moisture profile experiments		
small diameter product	$D_{eff} = 2.52$ e-10	

54
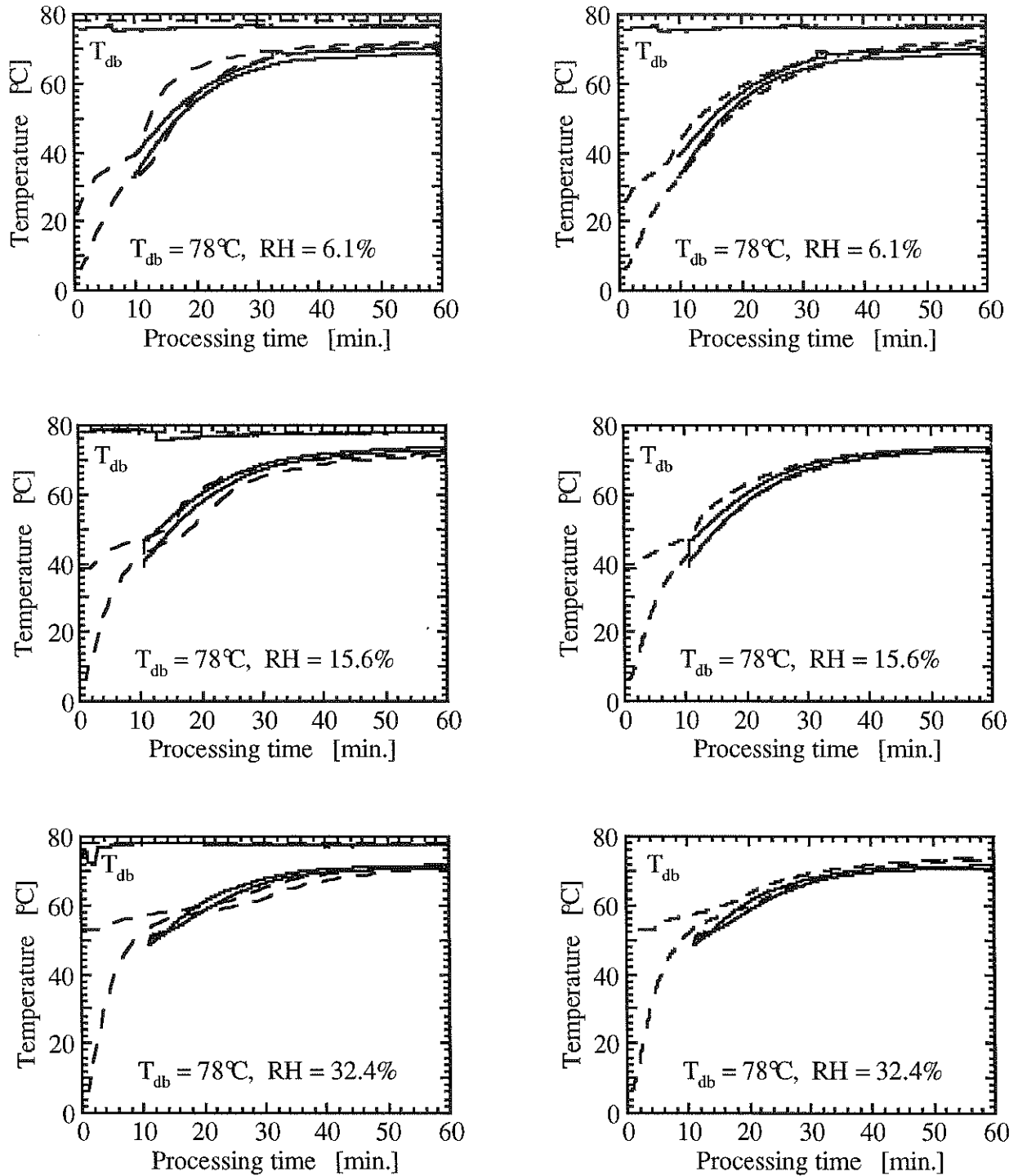
Figure 6.1: Simulated (dotted lines) and measured data (solid lines) for a small diameter
full-fat product. The left column shows the simulation of Schaefer, the right
column the EES simulation.
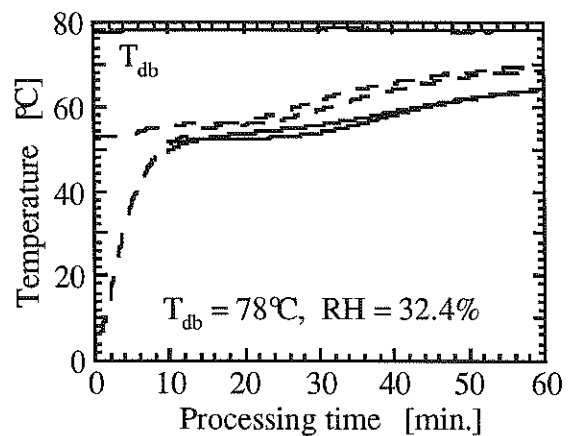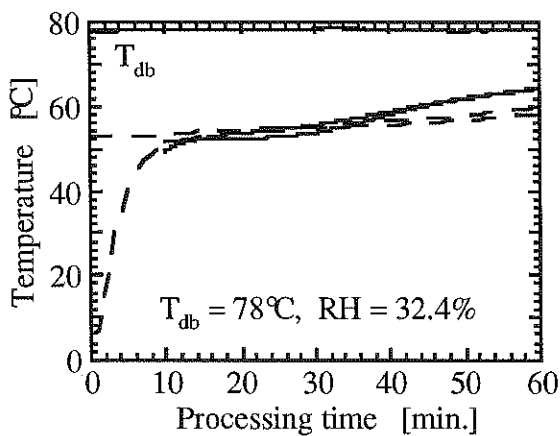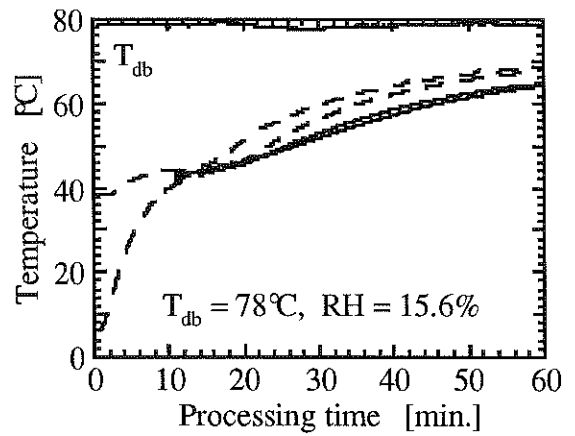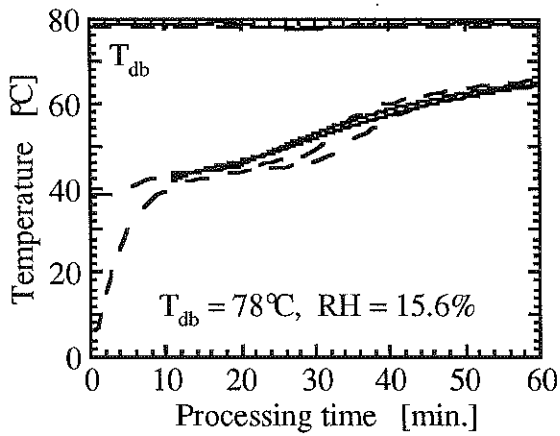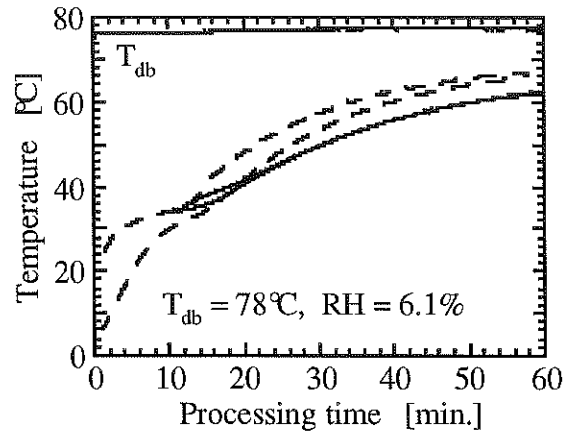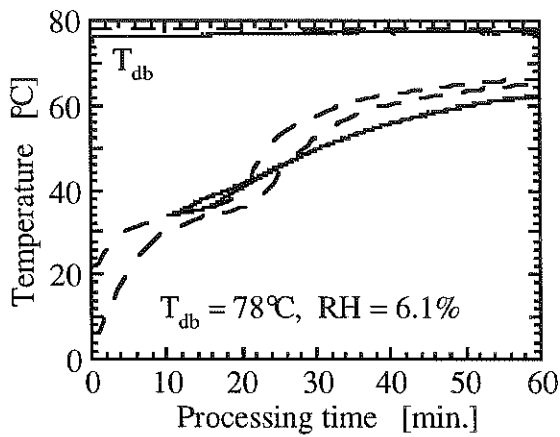
Figure 6.2: Simulated (dotted lines) and measured data (solid lines) for a small diameter no-fat product. The left column shows the simulation of Schaefer, the right column the EES simulation.

Figure 6.1 and Figure 6.2 show the simulated temperature profiles of a full-fat and no-fat product for the different process air conditions as listed in Table 6.2. The left columns show the simulation results of Schaefer, the right columns show the simulation results of the EES program. Both are compared to the measured temperature profiles. It can be seen that the error of the EES program is slightly smaller for the full-fat product, while the error of the no-fat product is higher. The FORTRAN simulation tents to underestimate the temperature for higher relative humidities, while the EES program tents to overestimate the temperature. The EES program does not offer the opportunity of an integrated parameter estimation program. But as long as the moisture diffusivity coefficient is the only unknown, a good parameter estimation can be made by trial and error.
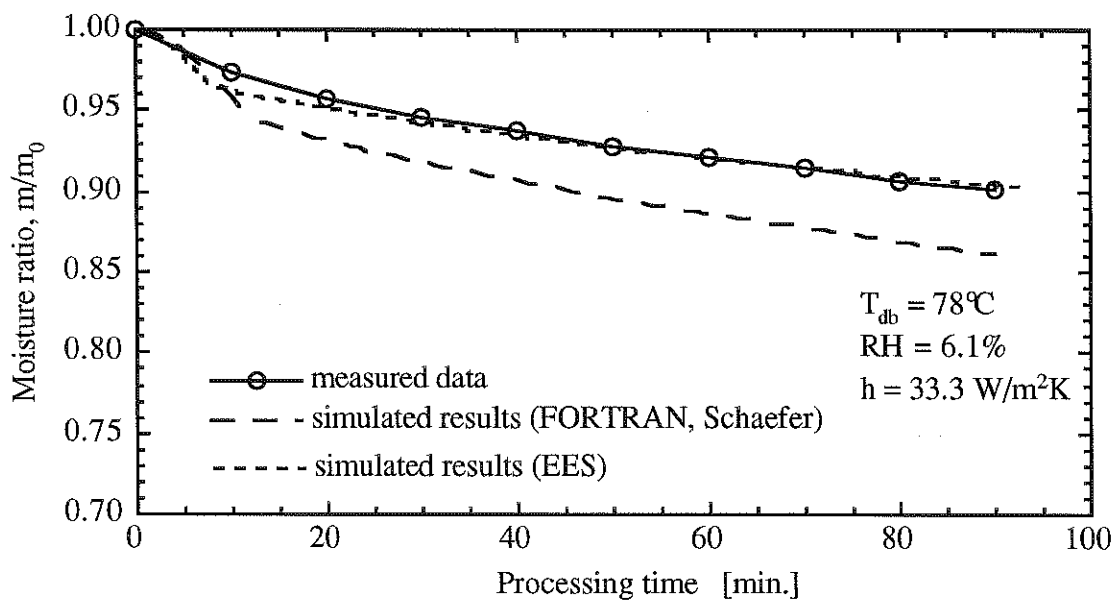
Figure 6.3: Simulated and measured moisture loss data for a full-fat meat emulsion product in a test section of a laboratory apparatus.
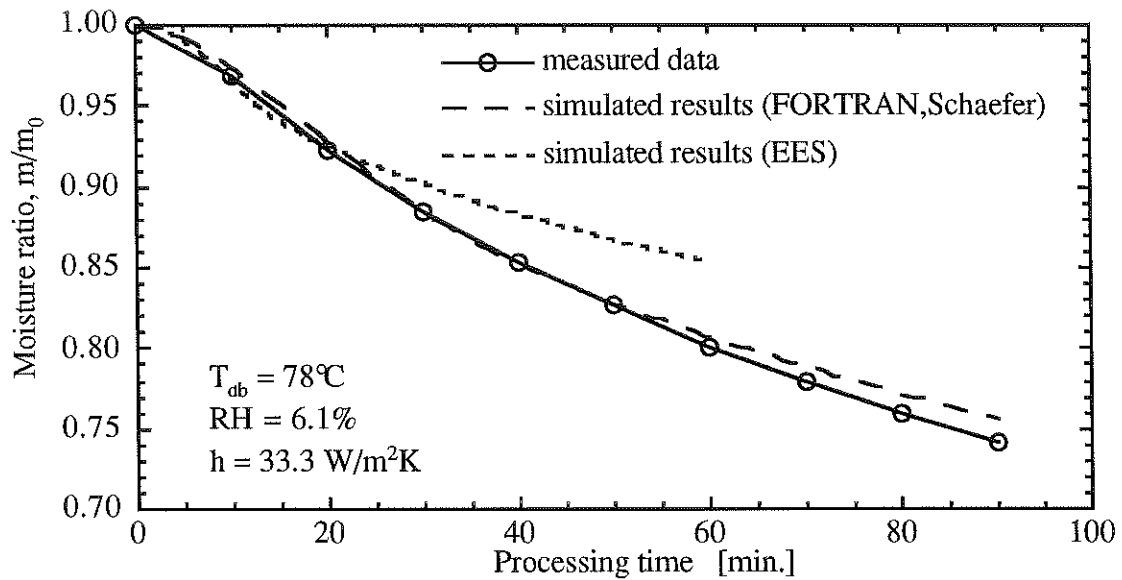
Figure 6.4: Simulated and measured moisture loss data for a no-fat meat emulsion
product in a test section of a laboratory apparatus.

Figure 6.3 and Figure 6.4 show the data of moisture loss experiments made by Schaefer
[1995]. They are compared to the simulation results of the FORTRAN simulation
(Schaefer) and the EES program. The EES program gives good results for the full-fat meat
emulsion product and underestimates the moisture loss of the no-fat meat emulsion
product. The low moisture loss is also a reason for the high temperatures of the simulated
no-fat product, because the evaporation heat losses are to small. It can be seen that the
simulations are close to the measured data in the fist 20 minutes of the process. The large
error of the moisture loss of the no-fat product can be avoided if a higher moisture
diffusivity coefficient is used. This will decrease the error of the calculated mass loss, but
might increase the calculated cooking time. Figure 6.5 shows the measured moisture

concentration profile for a 22 mm diameter product with an initial moisture content of $u_{ini} = $ 1.275 kg_m/kg_d and a moisture diffusivity coefficient of $D_{eff} = 2.52e\text{-}10\ m^2/s$.
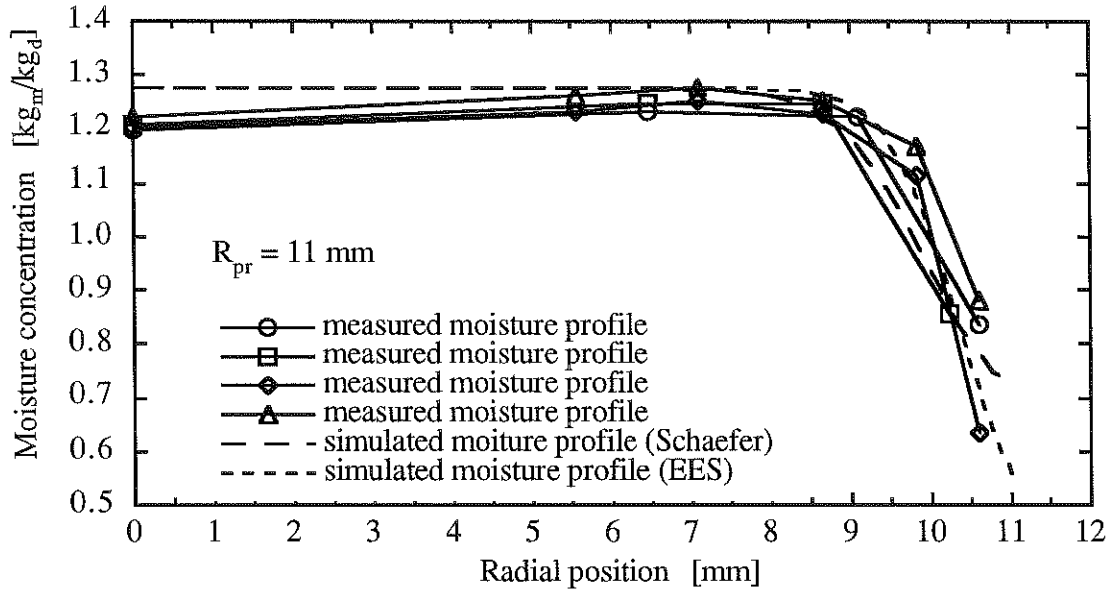
Figure 6.5:   Simulated and measured moisture concentration profiles for a full-fat meat emulsion product.

The simulated and measured data near the surface are in close agreement. The measured moisture concentration in the center of the product for some reasons is lower than the initial value. Schaefer assumed that this is a reason of an increasing error of the measurement towards the center of the product.

6.2 Process Simulation and Measured Data

The simulation program developed in this work is based on the models developed in Chapter 3. It is designed to calculated the temperature, the moisture content and the moisture loss of cylindrical meat emulsion products. Values of the model parameters that

do not change with different process conditions are listed in Table 6.1. For the moisture

diffusivity constant values are used as estimated by Schaefer [1995] and listed in Table 6.2.

Table 6.3:Parameter and data for the process simulation shown in Figure 6.3 to Figure 6.8.

Process Parameter					
	Time per zone[1] [min]	$T_{dry\ bulb}$ [C]	Relative Humidity RH [%]	Air velocity v [m/s]	Heat Transfer Coefficient h [W/m^2 K]
Spraying zone	12	40	100	1.1	16.8
Smoke zone	12	71	21.5	1.1	16.8
Drying zone	18	79	14.1	3.84	30.1
Dry cooking zone	12 (15)	73	54.6	3.84	29.9
Final cooking zone	18 (15)	82	70.4	3.84	29.3
Property Data					
	full-fat product		*non-fat product*		
	$D_{eff} = 1.48e\text{-}10\ m^2/s$ $\rho = 1023\ kg/m^3$ $\rho_d = 434\ kg/m^3$		$D_{eff} = 2.61e\text{-}10\ m^2/s$ $\rho = 1036\ kg/m^3$ $\rho_d = 135\ kg/m^3$		
Model Parameter					
	N = 15 $\Delta t = 10$ s				
Initial Conditions					
	full-fat product		*non-fat product*		
	$T_{ini} = 6C$ $u_{ini} = 1.358\ kg_m/kg_d$		$T_{ini} = 6C$ $u_{ini} = 6.692\ kg_m/kg_d$		

[1]The time given in brackets is the time period as interpreted from Fig.6.5 of Spielberg, the plain number are the time periods given by Schaefer

The smokehouse conditions for the standard thermal process as used by Spielberg and

Schaefer, the property data, model parameter and initial conditions for full-fat and non-fat

products are listed in Table 6.3. In the following figures T_{surf} and T_{center} are the temperature of the surface node and the center node of the product model. u_{center} is the moisture concentration in the surface node, T_{db} is the dry bulb temperature and T_{wb} is the wet bulb temperature of the process air.
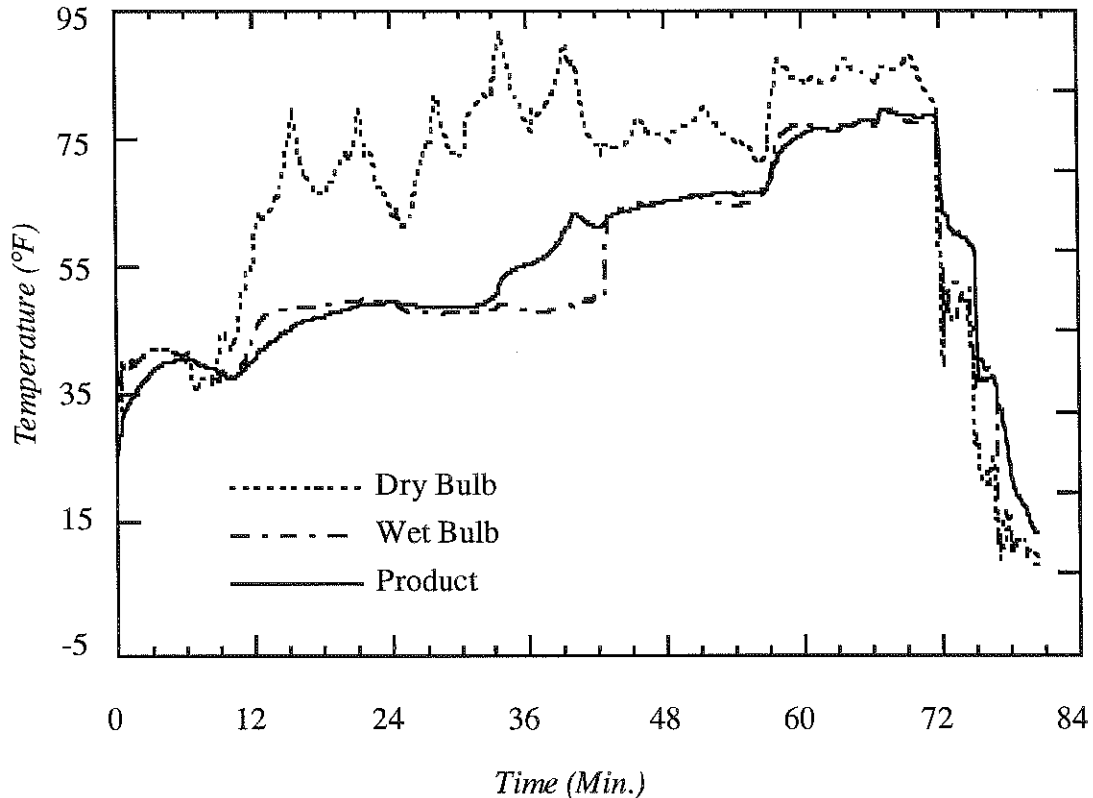
Figure 6.6: Measured product and process air temperatures of a continuos commercial smokehouse as reported by Spielberg[1992].

Figure 6.6 shows the temperature of a small diameter product measured by Spielberg [1992] in a commercial smokehouse process. The process consists of five zones: the spraying zone (12min), smoke zone (12min), drying zone (18min), dry cooking zone (15min) and the final cooking (15min).This temperature profile can be compared to the simulated process data for a full-fat and non-fat product shown in Figure 6.7 and Figure 6.8. They show the temperature at the surface and the center of the product and the surface moisture concentration.

Process simulation
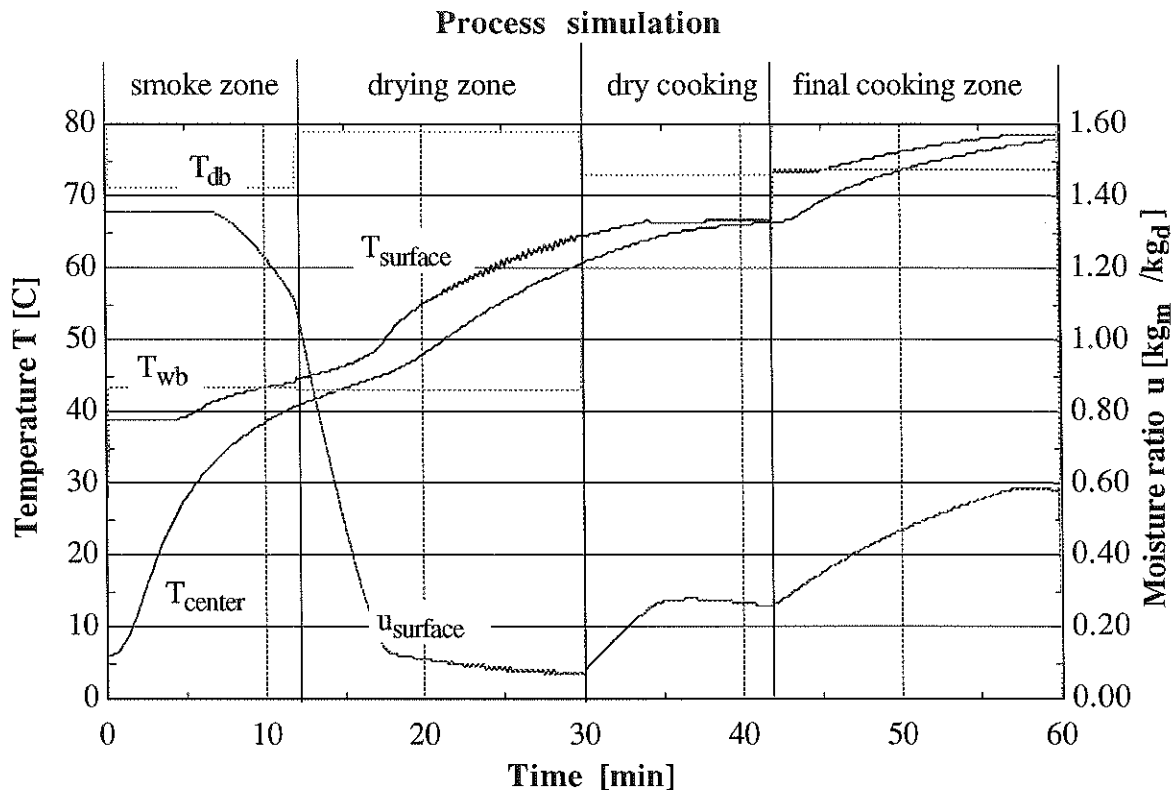
Figure 6.7: Simulated temperature profile at the surface and the center of the product and surface moisture concentration profile of a full-fat product.

The simulated processes have four zones starting with the smoke zone and the conditions given in Table 6.3 using the time period as interpreted from Figure 6.6. The simulation is unstable in the end of the drying zone due to the steep concentration gradient near the surface of the product and/or small variable changes. This can be avoid by using a smaller time step Δt for the simulation, thus this would cause problems due to the limited numbers of runs using EES it is neglected in these simulations. If a smaller time step is necessary, separate runs has to be made using a different program to save the data of the previous time period.

The temperature of the full-fat product increases faster than the temperature of the non-fat product due to lower moisture losses. Thus the temperature profile of the non-fat product is more similar to the measured data in Figure 6.6. The temperature is most of the time very close to the wet bulb temperature of the process air. It increases rapidly at the end of the drying zone and in the beginning of the final cooking zone. In the dry cooking zone changes in the product temperature are small. The temperature of the non-fat product increases slower, because the moisture loss and the moisture diffusivity coefficient are higher. The moisture ratio of the full-fat and non-fat product are shown in

Process simulation

$t_{cooking}$ = 46.3 min; m_{loss} = 7.5 %
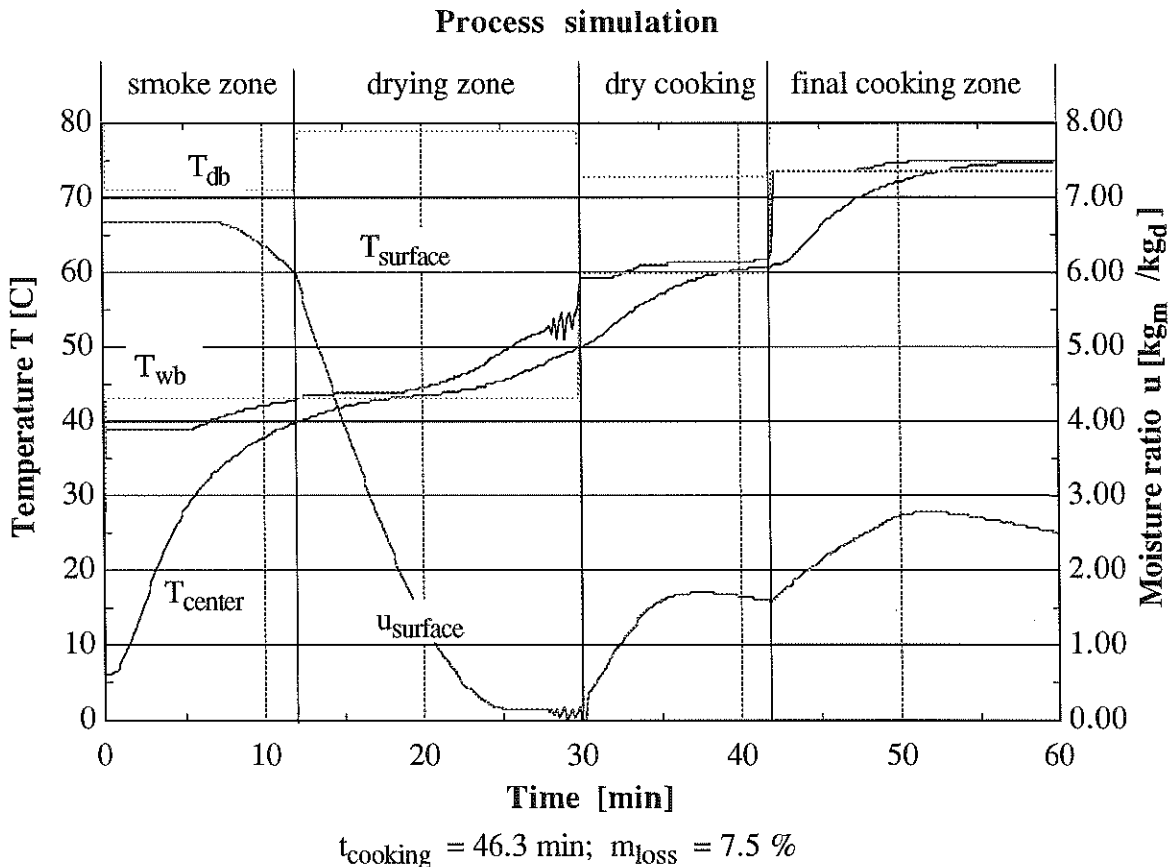
Figure 6.8:   Simulated temperature profile at the surface and the center of the product and surface moisture concentration profile of a non-fat product.

Figure 6.9. Thus the initial moisture content and the driving force for moisture transfer at the surface increase simultaneously it takes about the same time to dry the surface of the full-fat and non-fat product to the equilibrium moisture content of about 0.2 kg_m/kg_d. In the dry cooking zone and the final cooking zone the moisture content of the surface will increase again. This is a reason of moisture diffusion from the center to the surface of the product. While the high moisture gradient near the surface increases the driving force of mass transfer from the center to the surface, the higher relative humidity in the dry cooking zone and final cooking zone decrease the driving force from the surface to the process air.
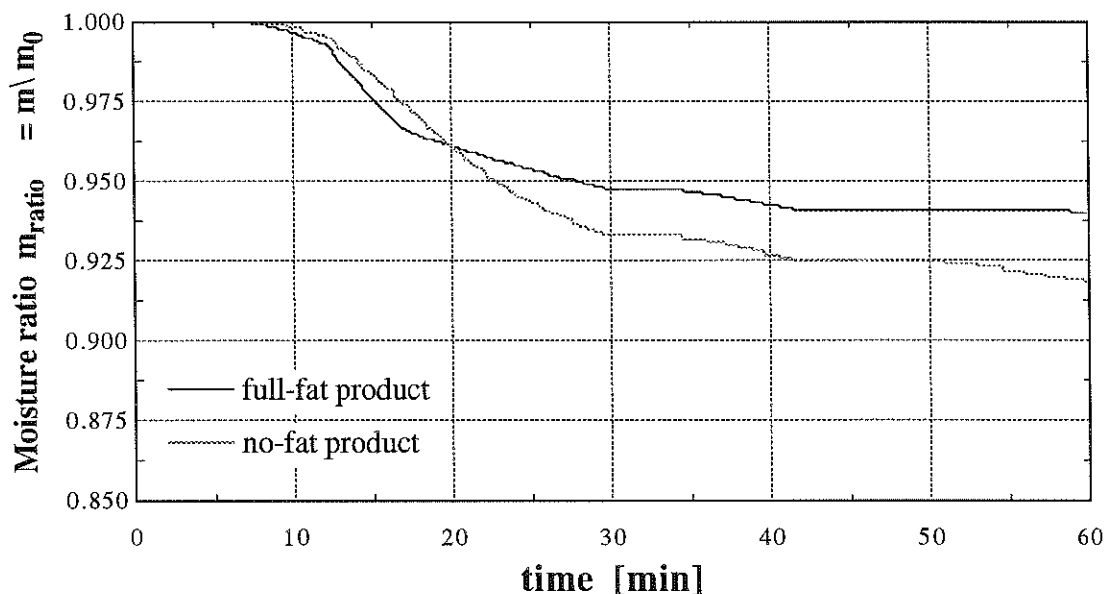
Figure 6.9:   Simulated moisture ratio for a full-fat and no-fat product.

Due to the higher relative humidity the required vapor pressure at the surface of the product will increase also and there will be no mass transfer before the temperature at the surface is high enough. This causes the steep increase of the moisture content at the surface of the product in the beginning of the last two zones. The moisture content decreases again when the surface temperature is high enough to evaporate the moisture at the surface. The

moisture loss at cooking time is 6.3% and 7.5% for the full-fat and no-fat product ,

respectively. In the end of the entire thermal process the moisture loss is 6.3% and 8%.

The moisture concentration profiles of the full-fat and non-fat products at the end of each

zone are shown in Figure 6.10. After the first two zones (30 min.) a steep concentration

gradient has developed at the surface, that relaxes in the third and fourth zone.

Moisture concentration as a function of time and position
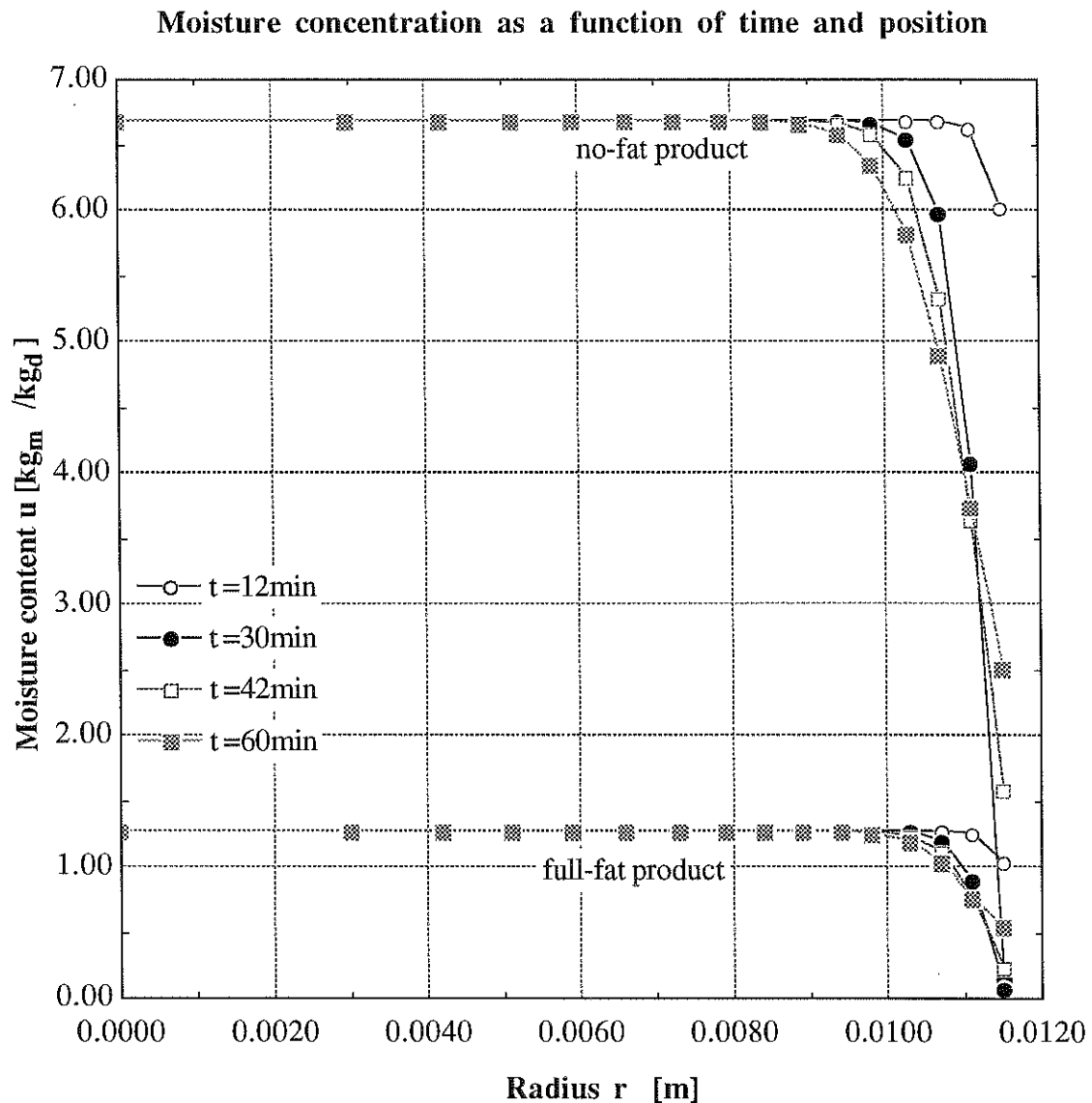
Figure 6.10: Moisture concentration profile for a full-fat and no-fat product at the end of
each smokehouse zone for the conventional process.

The penetration depth of the drying process increases constantly during the process. One can see that the change of the concentration profiles during the process are very similar. The penetration depth of the non-fat product is deeper and concentration gradient in the end of the drying zone is significant steeper for the non-fat product, that has a higher initial moisture content.

6.3 Improvements

Modern thermal meat emulsion processes have significant shorter process times as shown in Table 6.4. The changes in the process conditions that are necessary to shorten the cooking time are discussed in this paragraph. Tabel 6.4 also gives the new process conditions as chosen after several tries. The previous values are given in brackets if they have changed.

For the new processes the heat transfer coefficients and the temperatures can be as high as 40 W/m^{2}K and 104°C, respectively. Higher temperatures are necessary to guaranty the health requirements even for shorter process times. It is reported, that even with shorter process times the moisture loss is about 7%. The main changes have to be made in terms of air velocity, that means in terms of higher heat transfer coefficients. As shown in Table 6.4 the heat transfer coefficient in all zones is between 30 W/m^{2}K and 40 W/m^{2}K. The highest heat transfer coefficient will occur in the drying zone to allow the skin to dry. Because of the low relative humidity, the temperature of the product in this zone does not rise significantly. The drying zone for the no-fat product is longer due to the higher moisture content and therefore larger moisture rate at the surface. The final cooking zone on the other hand is shorter, thus the higher moisture content provides a higher conductivity, so the product can be heated up faster if the moisture transfer is once finished. The drying zone also limits the temperature in the smoke zone. The temperature of the product should

Table 6.4:   Parameter an data for the improved thermal process as shown in Figure 6.11 to Figure 6.14.

	Time per zone[1] [min]	$T_{dry\ bulb}$ [C]	Relative Humidity RH [%]	Air velocity v [m/s]	Heat Transfer Coefficient h [W/m^2 K]
Process Parameter					
full-fat product					
Smoke zone	5 (12)	75 (71)	25 (21.5)	3.84 (1.1)	30.0 (16.8)
Drying zone	6 (18)	82 (79)	15 (14.1)	7.0 (3.84)	39.7 (30.1)
Dry cooking zone	8 (15)	75 (73)	54.6	3.84	29.9
Final cooking zone	7 (15)	104 (82)	60 (70.4)	7.0 (3.84)	34.4 (29.3)
Chilling zone	3 (-)	0 (-)	99 (-)	3.84 (-)	30.1 (-)
no-fat product					
Smoke zone	5 (12)	71	21.5	3.84 (1.1)	30.1 (16.8)
Drying zone	7 (18)	85 (79)	10 (14.1)	7.0 (3.84)	39.8 (30.1)
Dry cooking zone	8 (15)	75 (73)	54.6	3.84	29.9
Final cooking zone	6 (15)	104 (82)	60 (70.4)	7.0 (3.84)	34.4 (29.3)
Chilling zone	3 (-)	0 (-)	99 (-)	0.5 (-)	11.66 (-)

Property Data

	full-fat product	*non-fat product*
	$D_{eff} = 1.48e\text{-}10\ m^2/s$	$D_{eff} = 2.61e\text{-}10\ m^2/s$
	$\rho = 1023\ kg/m^3$	$\rho = 1036\ kg/m^3$
	$\rho_d = 434\ kg/m^3$	$\rho_d = 135\ kg/m^3$

Model Parameter

$$N = 15$$
$$\Delta t = 4.6\ s$$

Initial Conditions

	full-fat product	*non-fat product*
	$T_{ini} = 6C$	$T_{ini} = 6C$
	$u_{ini} = 1.358\ kg_m/kg_d$	$u_{ini} = 6.692\ kg_m/kg_d$

Process simulation
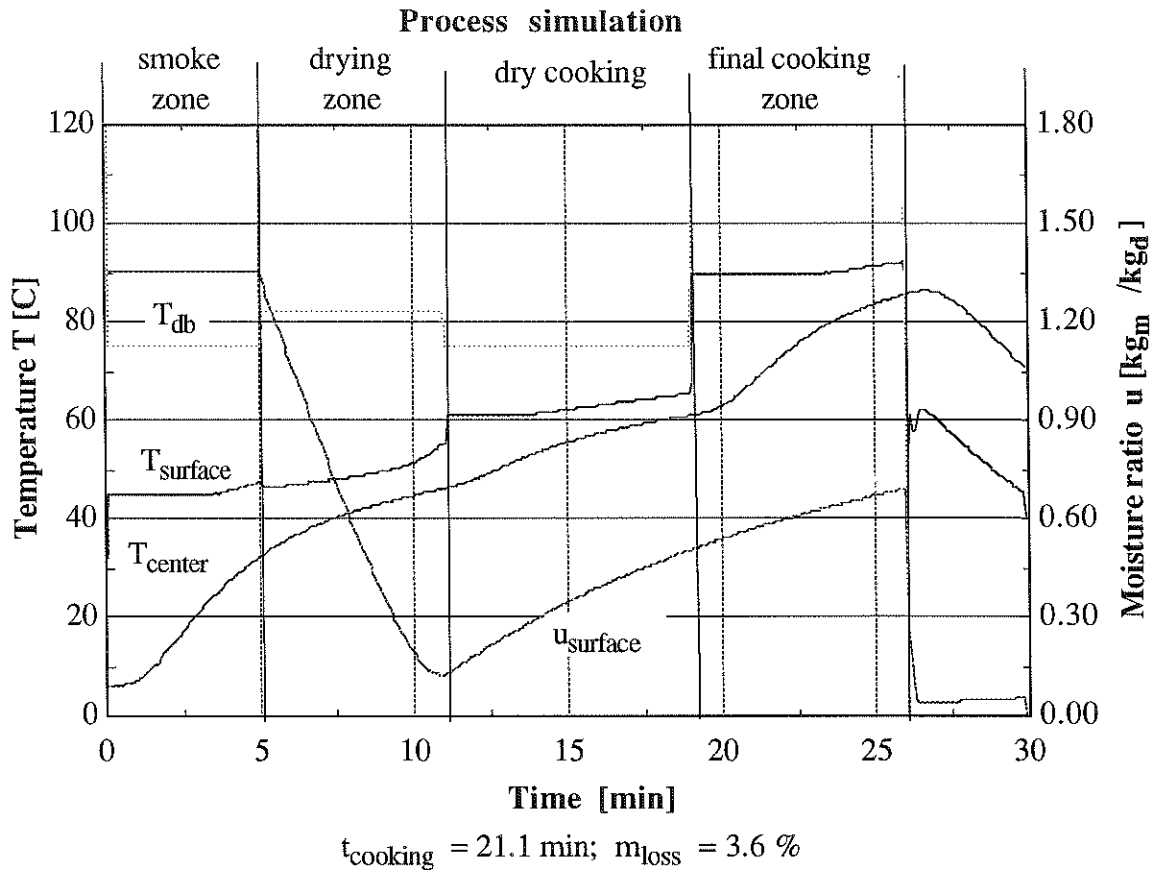
Figure 6.11: Improved thermal process of the full-fat small diameter heat emulsion product.

increase continuously during the whole cooking process. To avoid a temperature drop at the surface when traveling from one zone into the other, the wet bulb temperature has to be the same or higher in the following zone. Thus the relative humidity in the smoke zone is higher than in the drying zone, the dry bulb temperature in the drying zone needs to be lower than in the smoke zone.

The dry cooking zone is important in terms of the texture of the product. The product temperature should not rise above the cooking temperature of 68.3 °C and it should increase only slightly. Moisture loss also should be reasonable small. This is done by increasing the relative humidity to avoid moisture losses and lowering the dry bulb temperature and the heat transfer coefficient.

Process simulation

$t_{cooking}$ = 22.3 min; m_{loss} = 6.6 %
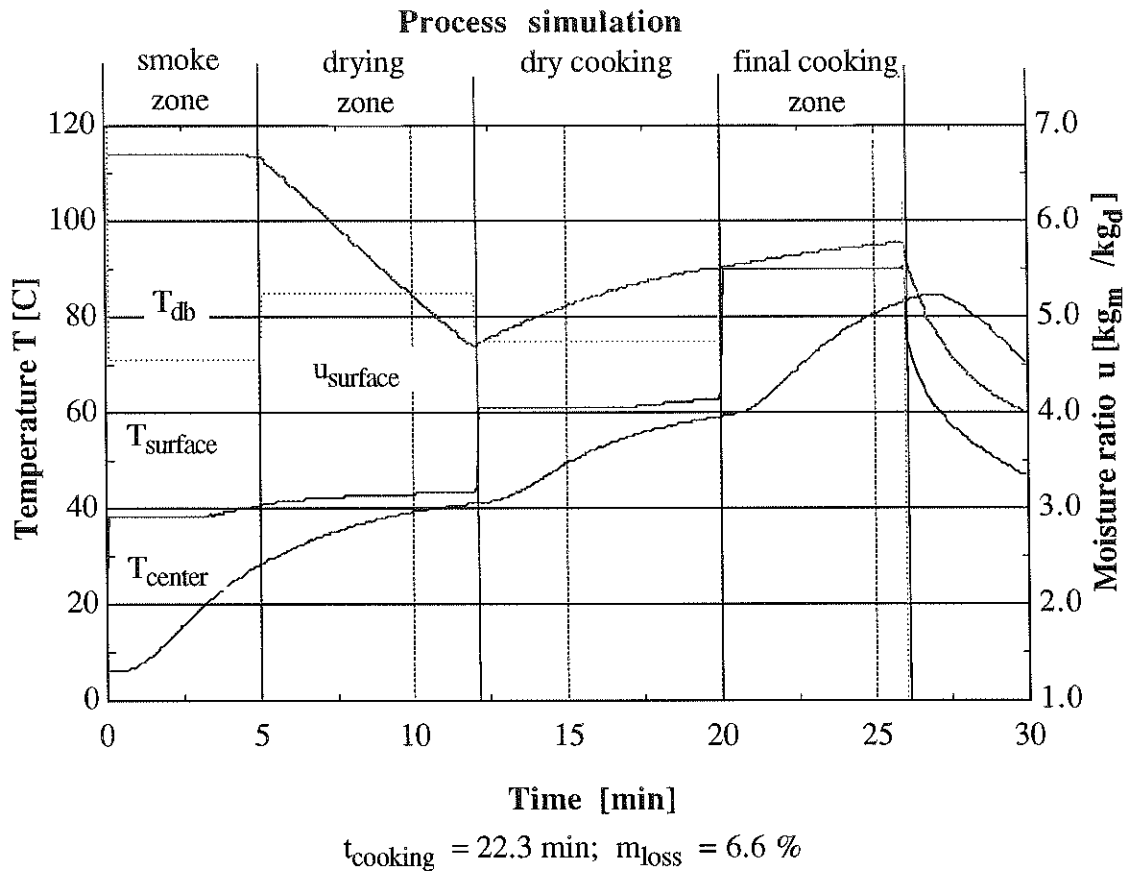
Figure 6.12: Improved thermal process of the no-fat small diameter heat emulsion product.

The final cooking zone is characterized by its high relative humidity and high temperature to increase the product temperature rapidly over the cooking temperature.

The moisture transfer for full-fat and no-fat products will take place in the drying zone only as shown in Figure 6.13. The moisture loss during the dry cooking and the final cooking zone is zero, as indicated by the constant moisture ratio. There will be moisture transfer in the chilling zone after the final cooking zone. This is a reason of the high vapor pressure at the product surface and the very low partial pressure of the moisture in the processing air even if a 100% relative humidity is assumed to account for the fact that cold water will be sprayed on the products.
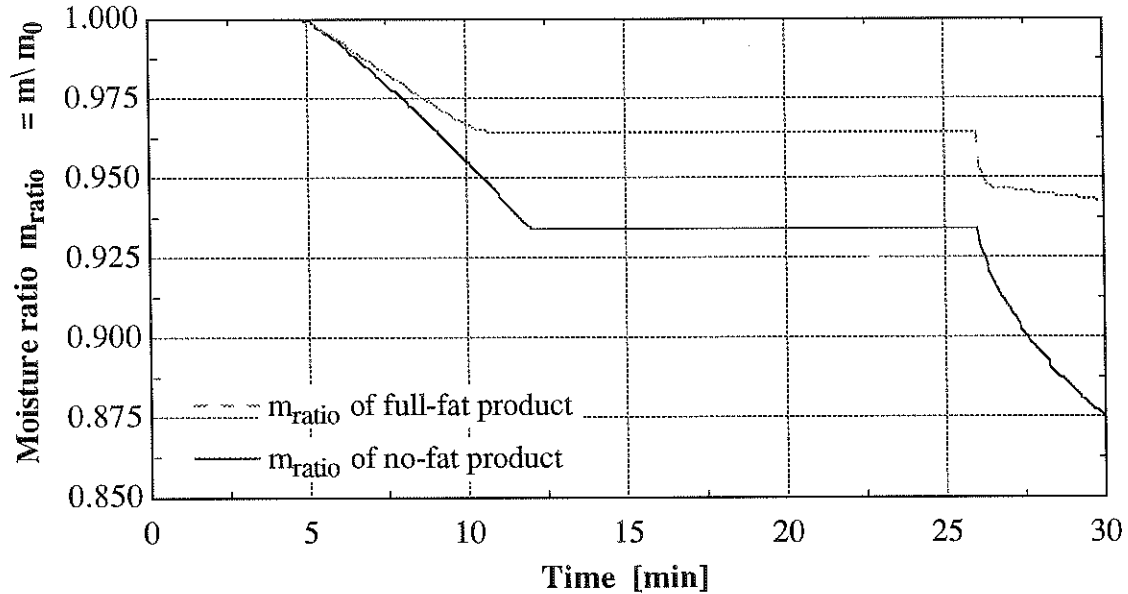
Figure 6.13: Moisture loss profile for the improved process for the full-fat and no-fat product.

Figure 6.14 shows the concentration profile of the full-fat and the no-fat product at the end of each process zone. The profile after 30 min process includes four minutes of chilling. Compared to the profiles of the conventional process in Figure 6.10 one can see that the penetration depth of the improved process is thinner. The concentration gradient at the surface of the no-fat product is also smaller for the improved process.

The processing of the no-fat product causes more difficulties, because the shorter drying process does not allow the surface to dry. This is indicated by the high surface concentration in the end of the process.
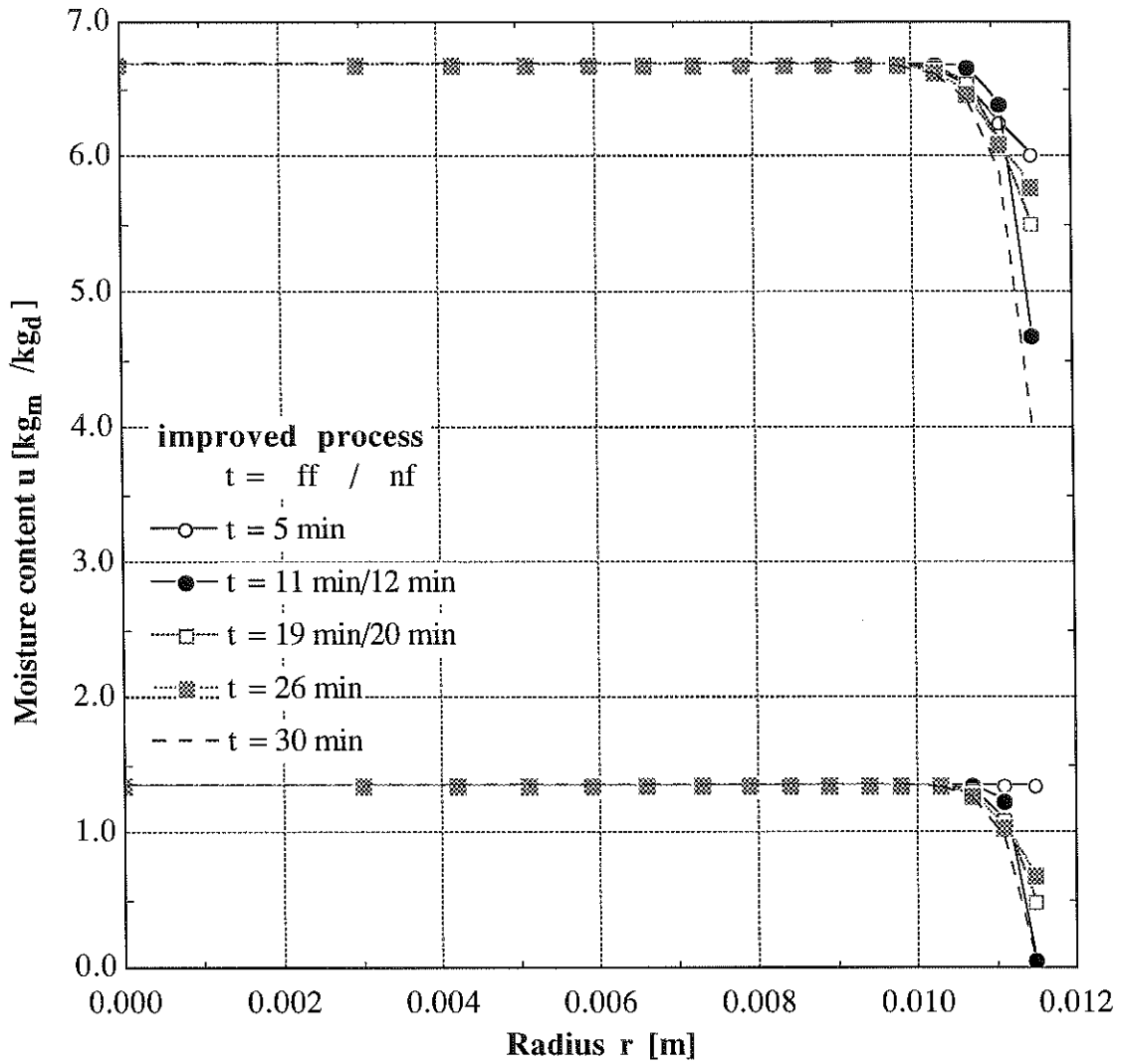
Figure 6.14: Moisture concentration profile for a full-fat and no-fat product at the end of each smokehouse zone for the improved process.

CHAPTER SEVEN

CONCLUSIONS AND RECOMMENDATIONS

This chapter will give a brief overview over the results of the simulation program developed in this work. Then it will recommend steps to improve the performance of the simulation program.

7.1 Conclusions

In this work a simulation model for heat and mass transfer in cylindrical meat emulsion products has been developed. It is based on several assumptions and simplifications introduced in Chapter 3. The most important assumptions are those of a one dimensional heat and mass transfer in radial direction and the assumption of moisture diffusion in liquid form. The implicit finite difference method is used to solve the differential equations. Furthermore models for the property data has been discussed and substituted in the model if the properties are dependent on the temperature and moisture concentration. The boundary conditions used in this work do allow moisture transfer from the product to the process air only.

The simulation program has shown the significant impact of the moisture diffusivity coefficient and the equilibrium isotherm between the surface moisture concentration and the relative humidity of the process air. The models available to predict the moisture diffusivity coefficient as a function of the temperature and moisture concentration failed to give

reasonable results. Thus the constant moisture diffusivity coefficients as estimated by Schaefer [1995] are used.

Using this model the temperature profiles and the moisture profiles and the moisture loss of full-fat product could be predicted accurately, while the simulated temperature and moisture profiles as well a the moisture loss of no-fat products are less accurate

7.2 Recommendations

The main problem by simulating the heat and mass transfer during the cooking process of meat emulsion products is the estimation of the diffusivity coefficient. Thus the value of the diffusivity coefficient significantly influence the moisture loss of the product and the cooking time. The EES simulation program used in this work does not offer the possibility of a parameter estimation program to calculate the moisture diffusivity coefficient. Further effort should be made to find a way to calculated or measure the moisture diffusivity coefficient.

As important as the moisture diffusivity coefficient of the product is the equilibrium isotherm between the product surface and the process air. The measured data used in this work give reliable information for dry moisture concentrations between $u = 0$ kg_m/kg_d and $u = 1$ kg_m/kg_d . For full-fat products the initial moisture concentration of the surface is $u = 1.5$ kg_m/kg_d and for no-fat moisture concentrations $u = 6.7$ kg_m/kg_d. In this work the equilibrium relative humidity for higher moisture concentrations is assumed to be constant $RH = 95$ %. Furthermore one curve-fit is used to represent the isotherm of the whole temperature range this also might be improved.

Using EES the number of runs per simulation is limited. This makes it difficult to use the program if a very small time step is required. Therefore the program should be transformed into FORTRAN and finally TRNSYS. A FORTRAN version of this model

already exists and can be improved. This might also be necessary for large diameter products when more nodes are necessary to simulate the heat and mass transfer, because a larger number of nodes reduces the available number of runs using EES.

APPENDIX A

EES PROGRAM

The EES program used in this work can be used for the simulation of the thermal processing of cylindrical meat emulsion products. It is designed to calculate the temperature and the moisture concentration of each node and the moisture loss of the total product.

To set the conditions of the process that needs to be simulated the process parameter, model parameter and property data has to be defined. This are altogether four block indicated with # signs in the beginning and the end of each block. For changes of the property data model as there is the conductivity, the specific heat or the moisture diffusivity, the currently used model needs to be replaced by a different model or a constant value.

Declaration of Variables

A_sec	effective cross section of the process zones, [m^2]
c_pfmol	specific heat of moist air; [J/mol K]
cp_air	specific heat of the process air; [J/kgK]
C_bar	average specific heat of the meat emulsion; [J/kgK]
C_d	specific heat of the dry product; [J/kgK]
C_w	specific heat of the moisture; [J/kgK]
dH	heat of evaporation; [J/kg]
dt	time step; [min]
dT_p	temperature difference between the surface and the process air; [C]

dV   volume of the internal nodes; $[m^3]$

D_ab   diffusivity coefficient of moisture in air; $[m^2/s]$

D_eff   effective moisture diffusivity; $[m^2/s]$

D_eff1   moisture diffusivity for T < 58C used in Model 2; $[m^2/s]$

D_eff2   moisture diffusivity for T > 58C used in Model 2; $[m^2/s]$

D_hyd   hydraulic diameter of the zone; $[m^2]$

D_sec   diameter of the section; $[m^2/s]$

FP   fat to protein ratio of the product used in Model 1&2; $[m^2/s]$

h   heat transfer coefficient; $[W/m^2\,K]$

i   node number; [-]

index   help variable; [-]

k_air   conductivity of the process air; [W/mK]

k_meat   thermal conductivity of the meat emulsion; [W/mK]

k_p   mass transfer coefficient at the surface of the product; $[kg/Pa\,m^2s]$

k_p'   help variable to determine k_p; $[kg/Pa\,m^2s]$

k_x   mass transfer coefficient; mole fraction driving force; $[mole/m^2s]$

L   length of the product; [m]

m_0   initial mass of moisture; [kg]

m_loss   moisture loss; [kg]

m_ratio   ratio of the current to the initial moisture content; [-]

mu_air   viscosity of air; [kg/m s]

MW   molecular weight, [g/mole]

N   total number of nodes

omega_m   wet-weight moisture concentration; $[kg_m/kg_t]$

p_air   partial vapor pressure of the process air; [kPa]

p_s_equ   equilibrium vapor pressure at the surface; [kPa]

P_kPa	process air pressure; [kPa]
Phi	dimensionless dry weight moisture concentration (for Model1); [-]
Pr	Prandtl number; [-]
q_v	convective heat flux towards the surface; [W/m^2]
q_d	conductive heat flux surface towards center; [W/m^2]
r''	radius of the surfaces of the nodes, [m]
r	radius of the center of the nodes; [m]
rho	total density of the product; [kg/m^3]
rho_air	density of air; [kg/m^3]
rho_d	dry density; [kg/m^3]
rho_m	moisture density; [kg/m^3]
R	radius of the product; [m]
Re	Reynolds number; [-]
RH	relative humidity; [%]
RH_equ_help	help variable to limit the equilibrium relative humidity; [%]
time	process time, [min]
T_cal	help value for the boundary condition procedure; [C]
T_db	dry bulb temperature; [C]
T_dp	dew point temperature; [C]
T_pr	initial temperature of the product; [C]
T_surf	temperature at the surface; [C]
Time#	travel time of the product after zone#; [min]
u_0	initial moisture concentration of the product, [kg$_m$/kg$_d$]
u_s	surface moisture concentration - dry-weight; [kg$_m$/kg$_d$]
v	air velocity; [m/s]
Zone#	time that the product stays in zone #; [min]

"################### Process Parameter ###############################"
Procedure Process(time:T_db,RH,v)

"Time spend in each zone (min)"
    Zone1 = 0   "Spraying"
    Zone2 = 5   "Smoke"
    Zone3 = 6   "Drying"
    Zone4 = 8   "Dry cooking"
    Zone5 = 7   "Final cooking"

"Travel time of the product:"
    Time1 = Zone1
    Time2 = Zone1+ Zone2
    Time3 = Zone1 + Zone2 + Zone3
    Time4 = Zone1 + Zone2 + Zone3 + Zone4
    Time5 = Zone1 + Zone2 + Zone3 + Zone4 + Zone5

"************** Zone 1 ****************"
  If (time <= Time1) Then
    T_db = 40
    RH = 0.99
    v = 1.1
  Else
"************** Zone 2 ****************"
    If (time> Time1) and (time <= Time2) Then
      T_db = 75
      RH = 0.25
      v = 3.84
    Else
"************** Zone 3 ****************"
    If (time > Time2) and (time <= Time3) Then
      T_db = 82
      RH = 0.15
      v = 7.0
    Else
"************** Zone 4 ****************"
      If (time > Time3) and (time <= Time4) Then
      T_db = 75
      RH = 0.546
      v = 3.84
    Else

```
"************** Zone 5 ****************"
            If (time > Time4) and (time <= Time5) Then
                T_db = 104
                RH = 0.60
                v = 7.0
            Else
"************** Zone 6 ****************"
                T_db =0
                RH = 0.99
                v = 3.84
            EndIf
          EndIf
        EndIf
      EndIf
  EndIf
End
"###########################################################################"


"* Calculation of the thermal conductivity  W/mK  ( M.Schaefer Table 2.2 page 15 ):   *"
Procedure k(N,i,index,omega_m:k_meat)
"Calculation of the thermal conductivity  W/mK  ( M.Schaefer Table 2.2 page 15 ):"
  If(omega_m>=0.6) and (omega_m<=0.8) Then
  k_meat := 0.08+0.52* omega_m
  Else
    If(omega_m<0.6) Then
    k_meat:=0.392
    Else
    k_meat:=0.496
    EndIf
  EndIf
End
"*******************************************************************"


"******   Flowchart for the surface temperature and the mass transfer coef.   ********"
```

"Procedure k_p" is the Procedure of the boundary conditions of the simulation model that DO NOT allow mass transfer to the product during the initial condensation period. This Procedure is based on the flowchart given by M.Schaefer Fig.3.2, p.51. The condensation period is the time in the beginning of the cooking process while the product temperature at the surface is lower than the dew point temperature of the process air."

```
Procedure k_p"(dT_p,T_dp,T_cal,q_v,q_d,p_s_equ,p_air,k_p:T_surf,k_p')
  If (dT_p < -1e-7) Then
    T_surf:=T_dp
    k_p'=0.0
    Else
       If ((dT_p >= -1e-7) and (dT_p < 0.1)) and (q_v < q_d) Then
          T_surf := T_dp
          k_p':=0.0
       Else
          If (p_s_equ < p_air) Then
            k_p':=0.0
            T_surf:=T_cal
          Else
            k_p':= k_p
            T_surf:=T_cal
          EndIf
       EndIf
  EndIf
End
"*************************************************************"
```

"Procedure D_eff" sets the boundaries for the moisture diffusivity model of Mittal [1982]"

```
Procedure D_eff"(D_eff1,D_eff2,T:D_eff)
  If (t<58) Then
     D_eff=D_eff1
  Else
     D_eff=D_eff2
  EndIf
End
"*************************************************************"
```

"*************** Equilibrium correction *************************"
"The curve fit to the measured data of Igbeka and Blaisdell alowes relative humidities above
100%. The following procedure"
"sets the upper limit to 95%"

```
Procedure Equil.correction(u_s,RH_equ_help:RH)
  If (RH_equ_help >= 0.95) Then
     RH := 0.95
  Else
     RH := RH_equ_help
  EndIf
End
"*************************************************************"
```

```
"*****************       Process Paramete   *****************************"
Call Process(time:T_db,RH,v_air )
P_kPa=101.325   "[kPa]"
"********************************************************************"


"#################   Simulation Parameter  ############################"
N=15
dt=4.6 "[sec]"
time=index*dt/60
"####################################################################"


"#################    Product Properties  ############################"
R=11.5e-3    "[m], diameter of the product"
L=15.2e-2    "[m] , lenght of the product"
T_pr=6.0     "Initial temperature of the product [C]"
u_0=1.5      "Initial moisture content of the product [kgm/kgd]"
FP=1.5       "Fat protein ratio of the product"



"The total density rho, the dry density rho_d and the moisture density rho_m of the meat
product:"
 rho=1024      "[kg/m^3]"
 rho_d=434   "[kg/m^3]"
 rho_m = rho - rho_d


"####################################################################"


"#################    Smokehouse data    ############################"
"Calculation of the hydr. diameter as postulate in M. Schaefer (datei:
apparatus.with.Nu.and.Re) based on the experiments. Note that this has to be checkt with
the actual size of the process stove. In this case the data of the test section are used to
calculate the hydr. diameter, the Reynolds number and heat transfer coefficient
respectivly."
D_hyd=2*A_sec/(pi*D_sec+pi*2*R)
D_sec=0.05 "[m]"
A_sec=pi/4*(D_sec^2-(2*R)^2)   "[m^2]"
"####################################################################"
```

"********************   Properties of moist air/water   ********************"
MW=0.018   "[kg/mole]"
dH=(3165-2.426*(tablevalue(index,#T[N])+273))*1000

rho_air=1/Volume(AirH2O,T=T_db,P=P_kPa,R=RH)   "[kg/m^3]"
k_air=Conductivity(AirH2O,T=T_db,P=P_kPa,R=RH)   "[W/m-K]"
cp_air=1000*SpecHeat(AirH2O,T=T_db,P=P_kPa,R=RH) "[J/kg-K]"
mu_air=Viscosity(AirH2O,T=T_db,P=P_kPa,R=RH)   "[kg/m-s]"
Re=v_air*D_hyd*rho_air/mu_air
Pr=mu_air/rho_air/alpha
alpha=k_air/rho_air/cp_air
{Calculation of the Lewis number}
Lewis=alpha/D_ab

"Diffiusion coefficient: M.Schaefer equation 5.19"
D_ab=0.281e-4*((T_db+273)/298)^(2/3)   "[m^2/s]"

"specific heat of moist air in J/mol-K for P=101.325 kPa and T=80 C"
c_pfmol=29.0+15.6*RH+0.967*RH^2+10.0*RH^3

"Nusselt correlation for a cylinder in crossflow (40< Re < 4000)"
h*(2*R)/k_air= C_Nu'*Re^m_Nu'*Pr^(1/3)   "[W/m^2-K]"
C_Nu'=0.683
m_Nu'=0.466
"***"

"******   Calculation of the initial mass and the mass loss of the product   *********"
 m_0=pi*R^2*L*rho_m
 dm_loss=2*pi*R*L*k_p*(p_s_equ-p_air)*dt
 m_loss=tablevalue(index,#m_loss)+2*pi*R*L*k_p*(p_s_equ-p_air)*dt
 dm_ratio=dm_loss/m_0
 m_ratio=(m_0-m_loss)/m_0
"**"

"/////////////////////////////////////// Parameter Models ///"

"********************   Specific Heat   *******************************"
"Calculation of the speciffic heat of the producd C_bar with the specific heat of the dry product C_d and of the water C_w[J/kg-K]"
C_d=1580   "[J/kg-K]   Specific heat of the dry product"
c[0]=757.1
c[1]=-11.56
c[2]=7.0838e-2
c[3]=-2.1655e-4
c[4]=3.3019e-7
c[5]=-2.0088e-10

    Duplicate i = 0,N
       "Specific heat of the meat emulsion   [J/kg-K]"
       C_w[i] = sum(c[k]*(tablevalue(index,i+3)+273)^k,k=0,5)*1000
       C_bar[i] = omega_m[i]*C_w[i]+(1-omega_m[i])*C_d

       "Wet-weight moisture concentration (mass fraction):"
       omega_m[i]=tablevalue(index,4+N+i)/(1+tablevalue(index,4+N+i))
    End
"**"

"*********************   Moisture Diffusivity   **********************"
" Calculation of the moisture diffusion coefficient [m^2/s] (ASAE Paper 80-6511, Mittal[1981])"
    Duplicate i=0,N
"*******************   constant   ***********************"
       D_eff[i]=1.48e-10 "[m^2/s] if D_eff is constant"
"*******************   Model 1 Mittal[1981] ***************"
       {D_eff[i]=0.0029*exp(-0.4419*FP-
4892.7/(tablevalue(index,3+i)+273)+11.55*Phi[i])/3600
            Phi[i]=(u[i]-u_equ)/(u_0-u_equ)}
"*******************   Model 2 Mittal[1982] ***************"
       {Call D_eff"(D_eff1[i],D_eff2[i],tablevalue(index,i+3):D_eff[i])
       D_eff1[i]=0.3224e-4*T_D_eff[i]*exp(-0.3302*FP-3060.37/T_D_eff[i])/3600
       D_eff2[i]=0.232*T_D_eff[i]*exp(-0.0414*FP-6246.6/T_D_eff[i])/3600
       T_D_eff[i]=tablevalue(index,i+3)+273.15}
    End
"***"

"************ Calculation of the heat and mass transfer analogy ***********"
"With the following equations the mass transfer coefficient is calculated as a function of the conditions of the processing air"
{k_x [moles/m^2-s] is based on a mole fraction driving force
k_p [kg/m^2-Pa-s] is based on a vapor pressure driving force}

{Equation (21.2-34) in Bird, Stewart, Lightfoot}
    h/k_x=c_pfmol*(Lewis)^(2/3)
{Relation between k_x and k_p}
    k_p'=k_x*MW/P_kPa   "[kg/kPa-m^2-s]"
"***"
"****** Calculation of the vapor partial pressure and equilibrium partial pressur ****"
"Calculation of the vapor pressure/humidity ratio in the air and at the surface of the product"
    p_w_sat=Pressure(Steam,T=T_db,x=1.0) "Vapor partial pressure of the process air"
    p_air=RH*p_w_sat "Partial pressure in the process air"
    p_s_equ=RH_equ*Pressure(Steam,T=tablevalue(index,#T[N]),x=1.0)
    T_dp=DewPoint(AirH2O,T=T_db,P=P_kPa,R=RH)"Dew point temperature of the air"
        "T_wb=WetBulb(AirH2O,T=T_db,P=P_kPa,R=RH)"
"Calculation of the equilibrium humidity ratio at the surface of the product with a curve fit to measured data from Igbeka "
"Blaisdell [1982]"
        Call Equil.correction(u_s,RH_equ_help:RH_equ)
        u_s=tablevalue(index,#u[N])
        u_s=sum(a[i]*RH_equ_help^i,i=1,5)
        a[1]=1.0802
        a[2]=-8.3266
        a[3]=30.65
        a[4]=-48.919
        a[5]=28.408
"***"
"************** Calculation of the sections within the product ***************"
"Calculation of the different radii r[i], dr[i], r'[j], dr'[j], r"[j]: With j=2*i, so that A_j=2*A_i. The radii r[i] describe the position of the center of the nodes.The radii r"[j] divide the cylinder in sections with equal volumes V/2 and the radii differences dr'[j] describe the boundaries of the node i."
r"[0]=0
r"[2*N]=R
    Duplicate j=1,2*N-1
        r"[j]=(j/2/N*R^2)^0.5
        dr'[j]=r"[j+1]-r"[j-1]
    End

```
Duplicate i=0,N
    r[i]=(i/N*R^2)^0.5
End
```

"Calculation of the equal volume differentials dV:"

dV=pi*R^2*L/N

"***"

"///////////////////////////// Calculation of tha Boundary Conditions /////////////////////////////////"

"*************** Heat flow into and out ot the surface node *******************"

```
dT_p=T[N]-T_dp
q_v=-h*dT_inf                        {q_v=-h*dT_inf   "Convectiv heat flux
from the process air to the product"}
q_d * dr'[2*N-1]= -dT_c[N]*k_N         {q_d=k_N*dT/dr "Conduction heat
flux from the center to the surface node"}
```
"***"

"** Calculation of the transient temperature profile using the explicit differential model **"

"Simplified B.C. for the center of the produced r=0 (i=0):"

```
Call k(N,0,index,omega_m[0]:k_0)
-2*k_0*pi*L*r'[1]*dT_c[0]/r"[2] =  rho*dV/2*C_bar[0]*dT_neu[0]/dt

-2*D_eff[1]*pi*L*r"[1]*du_c[0]/r"[2]=  dV/2*du_neu[0]/dt
```

"B.C. at the surface of the product r=R (i=N):"

```
Call k_p"(dT_p,T_dp,T_help[N],q_v,q_d,p_s_equ,p_air,k_p': T[N],k_p)
Call k(N,N,index,omega_m[N]:k_N)
dT_c[N]*2*k_N*pi*L*r"[2*N - 1]/dr'[2*N - 1] - 2*pi*r"[2*N]*L*h*dT_inf - 2*pi
*r"[2*N]*L*dH*k_p*(p_s_equ - p_air)  =  rho*dV/2*C_bar[N]*dT_neu[N]/dt

D_eff[N]*rho_d*pi*L*r"[2*N-1]*du_c[N]/dr'[2*N-1]-
2*pi*r"[2*N]*L*k_p*(p_s_equ -  p_air)  =  rho_d*dV/2*du_neu[N]/dt
```

"Internal i describes the position in the Hot Dog "

```
Duplicate i=1,N-1
    Call k(N,i,index,omega_m[i]:k_i[i])
1/r"[2*i]/dr'[2*i]*((k_i[i]*r"[2*i-1]*dT_c[i]/dr'[2*i-1] -
k_i[i]*r"[2*i+1]*dT_s[i]/dr'[2*i+1]) + C_w[i]*rho_d*T[i]*D_eff[i]*(r"[2*i-
1]*du_c[i]/dr'[2*i-1] - r"[2*i+1]*du_s[i]/dr'[2*i+1]))  =   rho*C_bar[i]*dT_neu[i]/dt
```

```
        D_eff[i]*pi*L*(r"[2*i-1]*du_c[i]/dr'[2*i-1] - r"[2*i+1]*du_s[i]/dr'[2*i+1])  =
    dV*du_neu[i]/dt
        End
    "**********************************************************************"


    "** Reading the temperatures out of the parametric table and calculated the differences  **"


    "T_idx_n, T_idx_s, T_idx_n describe the temperatures of the previeous time step. The
    indice n, s and c refere to "
    "n -the initial node;  s  - the node towards the surface and   c _ the node towards the
    center"


    "reading the center node"
        dT_c[0]= T[0]-T[1]
        dT_neu[0]=T[0]-tablevalue(index,#T[0])


        du_c[0]=u[0]-u[1]
        du_neu[0]=u[0]-tablevalue(index,#u[0])


    "reading the surface node"
        dT_c[N]= T[N-1]-T[N]
        dT_inf=T[N]-T_db
        dT_neu[N]=T_help[N]-tablevalue(index,#T[N])


        du_c[N]=u[N-1]-u[N]
        du_neu[N]=u[N]-tablevalue(index,#u[N])


    "reading the internal nodes"
        Duplicate i=1,N-1
          dT_c[i]=T[i-1]-T[i]
          dT_s[i]= T[i]-T[i+1]
          dT_neu[i]=T[i] - tablevalue(index,i+3)


          du_c[i]= u[i-1]-u[i]
          du_s[i]= u[i]-u[i+1]
          du_neu[i]=u[i] - tablevalue(index,i+N+4)
        End
    "**********************************************************************"
```

APPENDIX B

DATA

Table B.1: Moisture equilibrium data measured by Igbeka and Blaisdell [1982].

T = 5°C		T = 22°C	
u [kg$_m$/kg$_d$]	RH [%]	u [kg$_m$/kg$_d$]	RH [%]
0.000	0.00	0.000	0.00
0.018	10.53	0.032	11.58
0.025	20.00	0.049	21.75
0.028	30.18	0.056	31.23
0.032	43.16	0.076	43.51
0.058	59.65	0.112	61.05
0.100	74.39	0.175	75.44
0.189	81.05	0.337	80.35
0.351	84.91	0.628	83.86
0.589	88.42	0.912	88.07
0.842	91.93		
T = 38°C		**T = 55°C**	
u [kg$_m$/kg$_d$]	RH [%]	u [kg$_m$/kg$_d$]	RH [%]
0.000	0.00	0.000	0.00
0.049	9.82	0.088	10.53
0.074	21.75	0.119	21.75
0.084	32.98	0.133	32.28
0.102	42.91	0.14	42.91
0.140	61.05	0.175	60.35
0.217	72.98	0.274	72.98
0.393	78.60	0.414	75.79
0.554	79.65	0.710	80.70
0.821	84.56	0.933	84.21
1.025	87.37		

APPENDIX C

BIBLIOGRAPHY

Agrawal, Y., *Modeling and Experimental Analysis of Moisture and Heat Transport in Meat Emulsion Products during Smokehouse Thermal Processing* , PhD-Thesis, Ohio State University, 1976

Bird, R.B.; Stewart, W.E.; Lightfoot, E.N., *Transport Phenomena*, John Wiley and Sons, New York, 1960

Dickerson, R.W., " An Apparatus for Measurement of Thermal Diffusivities of Foods", *Food Technology* m **19**(5),198-204, 1965

Hallstöm, B ; Skjöldebrand, C., Träghårdh, C., *Heat Transfer and Food Products*, Elsevier Applied Science, Londen, 1988

Igbeka, J.C.; Blaisdell, J.L. ; "Moisture Isotherms of a Processed Meat Product - Bologna", *Journal of Food Technology* (1982) **17**, 37-46

Igbeka, J.C; Blaisdell, J.L.; "Simulation of moisture movement during drying an starchy food product-cassava", *Journal of Food Technology* (1982) **17**, 27-36